Stem Cell Reports
Report
OPEN ACCESS

Efficient Precision Genome Editing in iPSCs via Genetic Co-targeting with Selection

Katie A. Mitzelfelt,[1,10] Chris McDermott-Roe,[2,3,10,*] Michael N. Grzybowski,[2,3] Maribel Marquez,[2,3] Chieh-Ti Kuo,[2] Michael Riedel,[4] Shuping Lai,[2] Melinda J. Choi,[2] Kurt D. Kolander,[2] Daniel Helbling,[5] David P. Dimmock,[5] Michele A. Battle,[6] Chuanchau J. Jou,[7,8] Martin Tristani-Firouzi,[7,8] James W. Verbsky,[9] Ivor J. Benjamin,[1,2,11] and Aron M. Geurts[2,3,11,*]

[1]Department of Biochemistry, University of Utah, Salt Lake City, UT 84112, USA
[2]Cardiovascular Center
[3]Department of Physiology
Medical College of Wisconsin, Milwaukee, WI 53226, USA
[4]PharmaCell, 6229 Maastricht, the Netherlands
[5]Division of Genetics, Department of Pediatrics, Human Molecular Genetics Center
[6]Department of Cell Biology, Neurobiology and Anatomy
Medical College of Wisconsin, Milwaukee, WI 53226, USA
[7]Nora Eccles Harrison CVRTI, University of Utah School of Medicine, Salt Lake City, UT 84112, USA
[8]Division of Pediatric Cardiology, University of Utah School of Medicine, Salt Lake City, UT 83113, USA
[9]Section of Quantitative Health Sciences, Department of Pediatrics, Medical College of Wisconsin, Milwaukee, WI 53226, USA
[10]Co-first author
[11]Co-senior author
*Correspondence: mcdec@mail.med.upenn.edu (C.M.-R.), ageurts@mcw.edu (A.M.G.)
http://dx.doi.org/10.1016/j.stemcr.2017.01.021

SUMMARY

Genome editing in induced pluripotent stem cells is currently hampered by the laborious and expensive nature of identifying homology-directed repair (HDR)-modified cells. We present an approach where isolation of cells bearing a selectable, HDR-mediated editing event at one locus enriches for HDR-mediated edits at additional loci. This strategy, called co-targeting with selection, improves the probability of isolating cells bearing HDR-mediated variants and accelerates the production of disease models.

INTRODUCTION

Programmable nucleases are seeing widespread application in the genome engineering field on account of their ability to permit precise genetic modifications in cell cultures and whole organisms. The CRISPR/Cas9 (CRISPR-associated) system (Bhaya et al., 2011) has attracted particular attention on account of its flexibility, ease of use, and cost-effectiveness compared with alternative nucleases (e.g., zinc-finger nucleases [ZFNs] and transcription activator-like effector nucleases [TALENs]). Approaches utilizing ZFNs, TALENs, and, increasingly, CRISPR/Cas9 for the creation of genetically modified induced pluripotent stem cell (iPSC) lines that can be converted into pertinent somatic cell types for exploration of contextually relevant pathophysiological states have become a go-to strategy for delineating variant/disease association (reviewed in Hockemeyer and Jaenisch, 2016). Precision genome editing typically involves incorporation of an exogenously supplied DNA donor with the desired variant, often containing one or more additional sequence incorporations to prevent nuclease re-cutting (Long et al., 2014), into the genome of the host cell via the homology-directed repair (HDR) pathway following a nuclease-mediated, double-strand break. Despite enhancements in the efficiency with which donor DNA can be incorporated into the genome, HDR-based editing in iPSCs using either vector- or single-stranded oligodeoxynucleotide (ssODN)-based donors occurs infrequently, often less than 1% (Soldner et al., 2011; Wang et al., 2014). Consequently, identifying a cell that bears a mutation of interest, which can entail extended maintenance, expansion, and analysis of hundreds of clonal populations, is laborious, expensive, and not readily scalable.

Increasing evidence suggests that HDR, which represents the lesser-used method of genome repair, is dependent on various cell-autonomous factors. Mitotic manipulation, temporal regulation of Cas9 expression, and suppression of the non-homologous end-joining (NHEJ) pathway have all been shown to enhance HDR editing in vitro to varying degrees (Gutschner et al., 2016; Lin et al., 2014; Maruyama et al., 2015; Yu et al., 2015). Selecting cells based on reagent delivery and integration of Cas9 into the genome have also been shown to enhance the frequency of HDR (Ding et al., 2013a, 2013b; Gonzalez et al., 2014). Elegant strategies have been devised to isolate precision-modified cells, including knockin of excisable selectable cassettes and serial enrichment of positive subfractions (Miyaoka et al., 2014; Yusa et al., 2011). Here we implemented a simple and adaptable method that

obviates chemical perturbation, avoids stable Cas9 expression, maintains inherent DNA repair competence, does not require additional time or equipment, and is applicable to mismatch repair-proficient cell systems. We envisaged a potential HDR-competence spectrum across any population of transfected iPSCs, whereby a small subpopulation would naturally be more receptive to the incorporation of donor DNA via HDR while other cells remain refractory. In such a receptive cell, multiple independent HDR events could occur simultaneously meaning, in theory, an HDR-based primary editing event to incorporate a selectable marker at one locus could be accompanied by one or more independent user-specified HDR-mediated edits at other loci. Hence, isolation of cells based on the primary, selectable modification would enrich for the secondary, passenger modification(s). The methodology outlined herein is conceptually analogous to strategies previously described for the selection of cells harboring NHEJ-mediated gene-disruption events (Liao et al., 2015; Moriarity et al., 2014) although we extend the principle for isolation of cells bearing HDR-mediated precision editing.

RESULTS AND DISCUSSION

To test our hypothesis, we devised and implemented a strategy that we refer to as co-targeting with selection (CTS). CTS involves simultaneous transfection of human iPSCs with (1) a nuclease and donor plasmid designed to incorporate, via HDR, an antibiotic-resistance cassette into the *AAVS1* safe harbor site (Sadelain et al., 2012) on chromosome 19, and (2) CRISPR/Cas9-based reagents and a cognate ssODN designed to introduce a variant of interest at a second locus, followed by maintenance in antibiotic-containing medium for approximately 10 days to select for resistant (and theoretically HDR-competent) clones (Figures 1A and 1B). Antibiotic-resistant colonies are then isolated, clonally expanded, and screened for knockin of the variant of interest. CTS does not alter the duration from transfection to isolation and analysis, but based on our experience and data reported herein, markedly enhances the representation of cells bearing passenger modifications (knockin alleles at the gene of interest) in the final population.

We first applied the CTS method to a single gene (*CRYAB*) in hB53 hiPS6 iPSCs (Riedel et al., 2014). Following transfection of a pre-validated *CRYAB*-specific single guide RNA (sgRNA)-expressing pX330 vector and ssODN donor template (for incorporation of the passenger modification) as well as a commercially available *AAVS1*-specific TALEN pair and puromycin N-acetyltransferase (pac)-containing donor vector driven by a constitutive promoter (for incorporation of the selectable modification), cells were treated with puromycin per our CTS protocol (to enrich for cells that underwent HDR, Figure S1), for 48 hr (to eliminate untransfected cells), or not at all (to mimic a selection-free system) (Figure S2). Clones were then harvested and analyzed via Sanger sequencing for modification at the gene of interest. The total number of editing events (NHEJ and HDR) was >7-fold greater in CTS cells relative to unselected cells and, crucially, the HDR/NHEJ ratio was >4-fold greater (Figure 1C, left panel, and Table S1). This corresponded to a ~40% likelihood of picking a precision-modified clone, both heterozygous and homozygous, from the final culture with CTS compared with 2% (no treatment) or 4% (transient puromycin treatment) (Figures 1C, middle and right panel, and 1D). Interestingly, we did not observe enhancement in donor incorporation following isolation of transiently transfected cells in this experiment, which may be due to the *pac* cassette presence on the *AAVS1* donor-targeting construct and not on the gene-specific nuclease (pX330) plasmid. Therefore, direct comparisons with published methods where selection is performed for transfection of the nuclease containing plasmid (Ding et al., 2013a, 2013b) and CTS were not performed in this study. These data suggested that selecting for HDR-receptive cells via a selectable modification significantly enriched for cells bearing passenger modifications (precision edit events) at the site of interest.

To benchmark the impact of CTS on HDR representation in a more quantitative manner and across multiple loci, we applied the workflow to a total of seven disease-associated variants across four different genes (*CRYAB*, *BAG3*, *LMNA*, and *MTERF4*) in two separate iPSC lines (hB53 hiPS6 and hB119 hiPS9) and analyzed editing outcomes via deep-sequencing. Following CTS, cells were pooled and deep-sequenced using the Illumina MiSeq platform. Average sequencing coverage following read trimming and quality filtering across all experiments was >150,000×, and the error rate was estimated to be less than 0.1%. We observed an average 3.7-fold (hB53 hiPS6) and 3.3-fold (hB119 hiPS9) increase in the total number of edits (HDR and NHEJ) across all loci with CTS compared with those without CTS (Table S2). Focusing on precision editing events and considering all seven variants, we observed an average 50-fold increase in HDR with CTS compared with those without CTS in both cell lines (Figures 2A–2C; Table S2). In support of our hypothesis that CTS enriches for HDR, we observed an overt shift in the balance between the two modes of repair such that the HDR/NHEJ ratio was enhanced on average 18-fold (hB53 hiPS6) and 27-fold (hB119 hiPS9) with CTS compared with those without CTS (Figures 2D–2F; Table S2). Considering all loci and both cell lines, the HDR rate following CTS was ~14%,

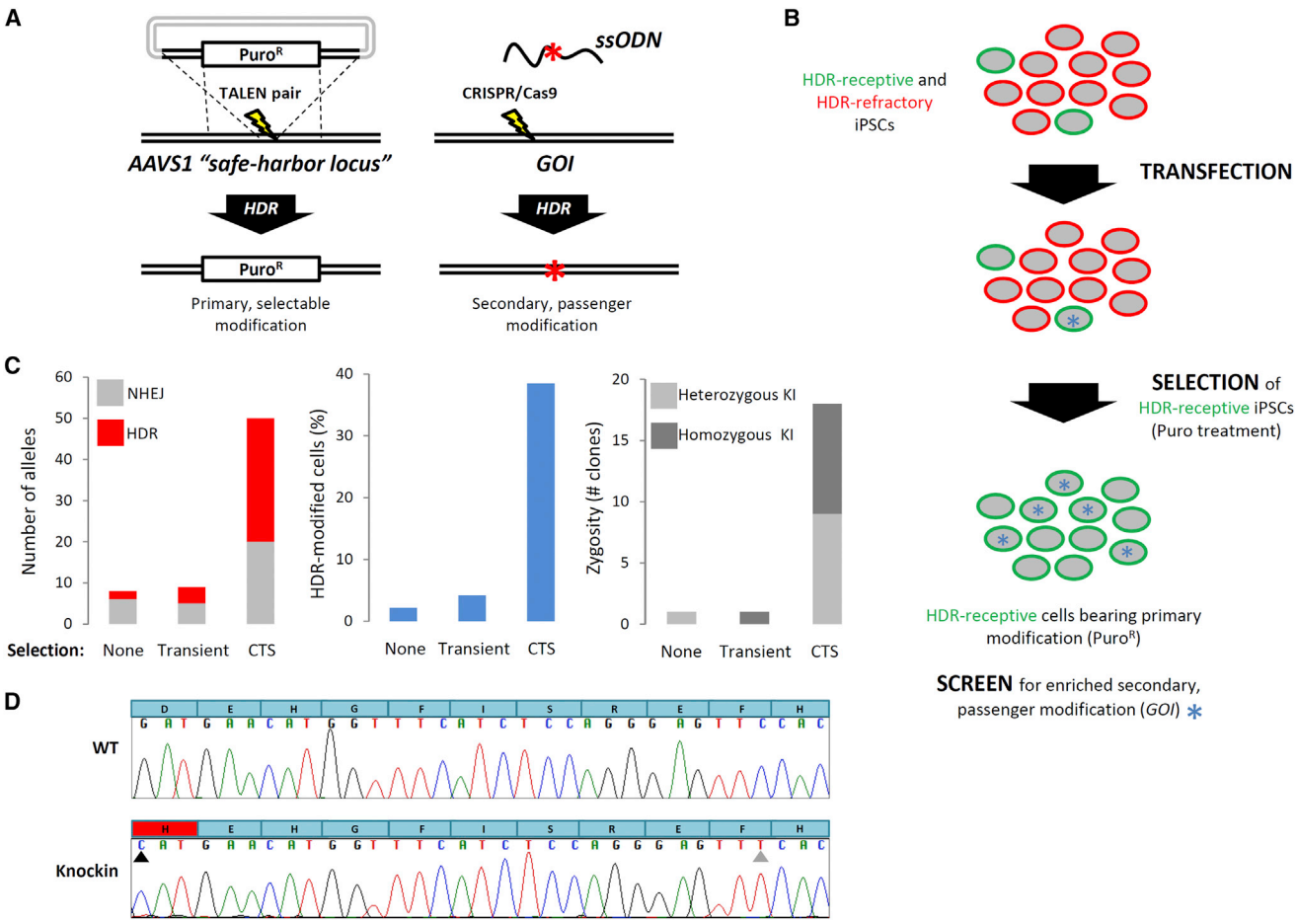

Figure 1. Rationale for CTS and Proof of Feasibility

(A) Cells are edited simultaneously with gene-specific CRISPR/Cas9 and ssODN containing a variant of interest (red asterisk) as well as plasmids expressing *AAVS1*-specific TALENs and a puromycin resistant (Puro^R) donor cassette.

(B) Components from (A) are transfected into iPSCs where HDR-receptive cells (green) are more likely to incorporate donor DNA than HDR-refractory cells (red).

(C) Precision-edited versus indel-containing alleles, detected via direct Sanger sequencing of relevant PCR products in hB53 hiPS6 iPSCs following CTS (n = 39) compared with no selection (n = 46) or transient exposure to puromycin (n = 48) (left panel), where n is the number of individual iPSC clones analyzed. Percent of clones bearing the *CRYAB*:c.325G>C variant (middle panel) and the number of heterozygous/homozygous clones (right panel).

(D) Representative chromatograms showing local *CRYAB* sequence of a wild-type (WT) clone (top) and that of a clone bearing a *CRYAB*:c.325G>C (homozygous) knockin allele (black arrow, c.325G>C variant; gray arrow, Cas9-blocking silent variant). See also Figures S1, S2, S4 and Table S1.

which corresponds to >1 in 10 clones bearing a precision edit.

While CTS led to a gross increase in incorporation of the intended passenger modifications, deep-sequencing data revealed significant variation in locus targetability. For example, representation of the *CRYAB*:c.343delT variant was 22% (hB53 hiPS6) and 25% (hB119 hiPS9) following CTS (1% [hB53 hiPS6] and 3% [hB119 hiPS9] without CTS), whereas representation of the *LMNA*:c.1346G>T variant was 1% (hB53 hiPS6) and 4% (hB119 hiPS9) HDR following CTS (<0.05% in both cell lines without CTS). Notwithstanding, the average >100-fold increase in HDR at *LMNA* with CTS means that isolating a precision-edited clone is feasible (~1 cell in 40 with CTS compared with ~1 cell in ~3,800 without, assuming heterozygosity) and suggests that loci which are inherently refractory to precision editing may be amenable via CTS. We also observed that the extent of ssODN incorporation was seemingly independent of its orientation relative to the sgRNA target strand (Table S3).

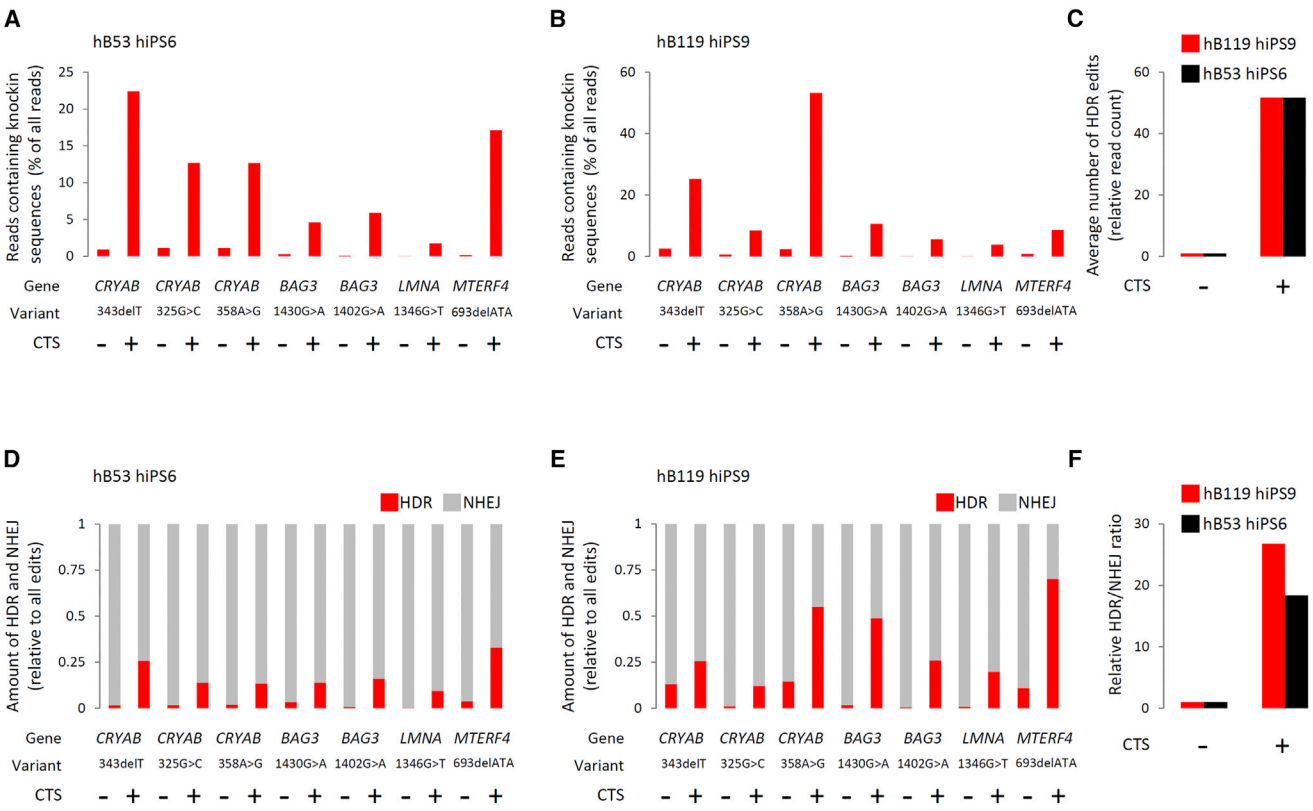

Figure 2. Quantitative Analysis of CTS-Enabled Precision Editing Across Multiple Genes

(A and B) Representation of precision (HDR only) editing events, based on read sequence and normalized to total read count, with (+) and without (−) CTS at multiple loci in hB53 hiPS6 (A) and hB119 hiPS9 (B) iPSC lines (−) CTS indicates cells handled in the same way as (+) CTS except for the addition of puromycin.

(C) Average fold change in HDR-mediated knockin with CTS relative to that without CTS, considering all loci in hB53 hiPS6 and hB119 hiPS9 iPSC lines.

(D and E) Relative proportions of reads bearing NHEJ- and HDR-based edits with (+) and without (−) CTS at multiple loci in hB53 hiPS6 (D) and hB119 hiPS9 (E) iPSC lines.

(F) Average increase in the HDR/NHEJ ratio in hB53 hiPS6 and hB119 hiPS9 iPSC lines with CTS relative to without CTS. See also Figure S3 and Table S2.

We next assessed how reflective the HDR editing rates calculated via deep-sequencing were of actual editing rates. Hence, the CTS protocol was repeated for all seven variants independently, and approximately 250 clonal populations were then picked and analyzed via Sanger sequencing. We successfully isolated cell lines for all seven mutations and observed a concordance between the quantities of HDR editing events determined via deep-sequencing and direct sequencing (Figures 3 and S3; Tables S2 and S3). We note that pooled deep-sequencing measures allelic representation at a specific time point and does not reflect zygosity or account for differing cellular growth rates from which the pool was derived. Extent of heterozygosity seemed to correlate, at least for the *CRYAB* mutations, with increasing distance from the CRISPR/Cas9 cut site (i.e., increased observation of heterozygous knockin clones with *CRYAB*:c.325G>C), but not in the case of *BAG3*:c.1430G>A, where we failed to isolate any mutant homozygous lines even though the targeted nucleotide was immediately adjacent to the CRISPR/Cas9 cut site. We speculate, as others have, that the nature and extent of zygosity is dictated by the distance between the CRISPR/Cas9 cut site and the targeted nucleotide as well as locus-dependent factors, such as chromatin organization (Paquet et al., 2016; Ward, 2015; Yang et al., 2013).

We analyzed the zygosity and specificity of *pac* cassette knockin at the *AAVS1* locus by Southern blotting and an integration-specific PCR assay (Figures S4A and S4B). We found that 50% of the clones (24/48) were correctly targeted without additional random integration. Of these, 21/24 were heterozygous and 3/24 were homozygous (Figure S4C). We observed

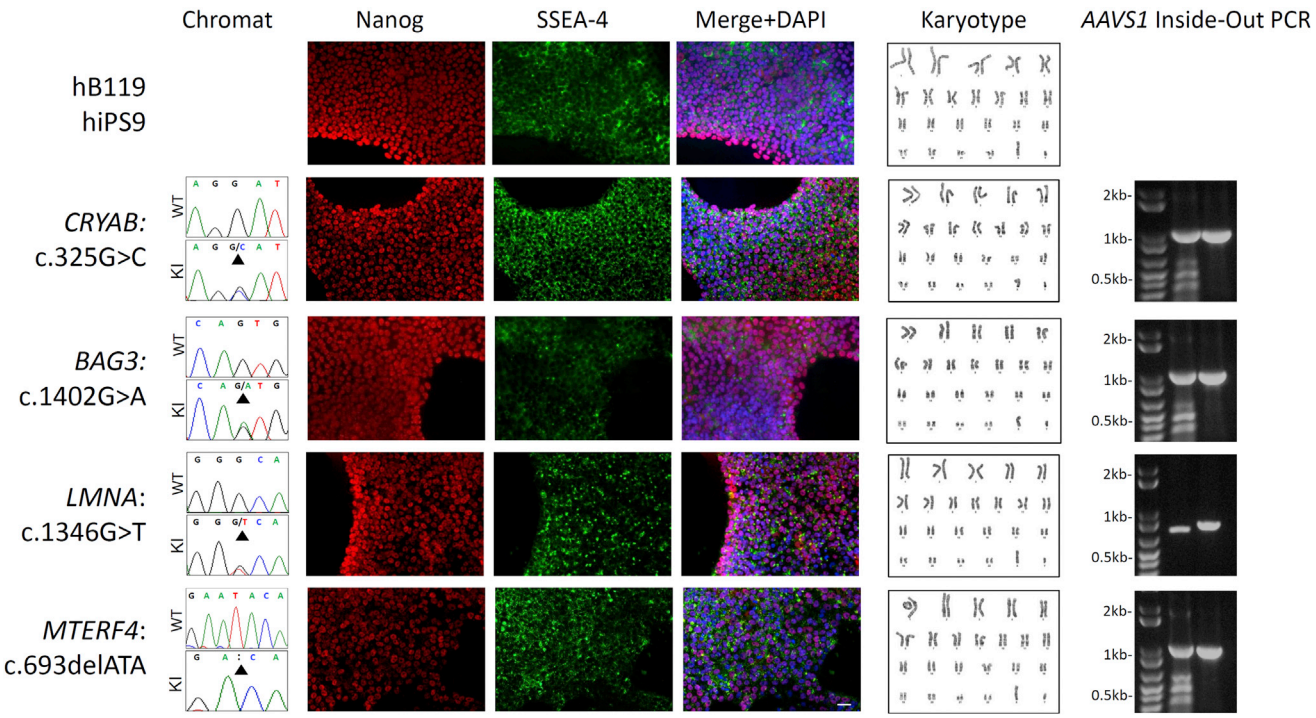

Figure 3. Validation of Knockin Cell Lines Generated with CTS

Knockin clones were generated for each disease-associated variant of interest shown in Table S3, with representative clones harboring variants in each gene shown here. Chromatograms (chromats) showing Sanger sequencing results of original cell line (WT) and knockin line (KI) with variants indicated by black arrows. Immunocytochemistry showing pluripotency markers Nanog and SSEA-4 for each knockin cell line harboring the respective variant of interest. Images were merged and counterstained with DAPI. Scale bar, 100 μm. Representative karyotypes for each cell line. Agarose gel showing *AAVS1* inside-out PCR for both the 5′ (middle lane) and 3′ (right lane) integration sites (Experimental Procedures), which demonstrates site-specific integration of the selection construct via HDR. See also Figure S3 and Table S3.

concordance between results from Southern blotting and the PCR-based assay. With the PCR-based assay, representative cell lines harbored the *pac* cassette at *AAVS1* (Figure 3) and none displayed evidence of additional aspecific integration events (data not shown). In addition, all lines analyzed exhibited the typical pluripotent cell morphology and karyotypic stability as well as expression of pluripotency markers (Figure 3), and maintained a capacity to form high-representation cardiomyocyte cultures (data not shown).

Despite improvements in sgRNA design (Doench et al., 2016), we nevertheless analyzed the top potential off-target sites (Experimental Procedures) in multiple mutant cell lines via Sanger sequencing and detected no signs of aspecific cleavage (data not shown). Furthermore, deep-sequencing of potential off-target sites (Experimental Procedures) revealed that CTS did not enrich for aberrant cutting compared with unselected cells (data not shown). The TALENs targeting *AAVS1* have been previously demonstrated to have minimal off-target cleavage (Hockemeyer et al., 2011). Collectively, these data suggest negligible reagent promiscuity and that while CTS enriches for cells bearing HDR-edited alleles, it does not enrich for off-target mutations. We note that GUIDE-seq (Tsai et al., 2015) or similar would be required for whole-genome examination of off-target cutting.

CTS is an inexpensive, rapid, straightforward, and readily scalable method, conceptually analogous to other marker-assisted enrichment strategies (Arribere et al., 2014), which increases the likelihood of isolating cells bearing knockin alleles by providing a non-integrating reporter of the HDR pathway activity akin to that devised by Flemr and Buhler (2015). While the precise cellular mechanisms of ssODN-mediated double-strand break repair remain to be elucidated, the observed enrichment by CTS via canonical homologous recombination of the double-stranded *pac* cassette donor into *AAVS1* suggests a transient state of HDR permissiveness and a potential overlap in these repair mechanisms in iPSCs. We encountered significant variability in inter-locus targetability and suspect that local sequence composition and chromatin organization likely influence repair preference. Given the multifactorial nature

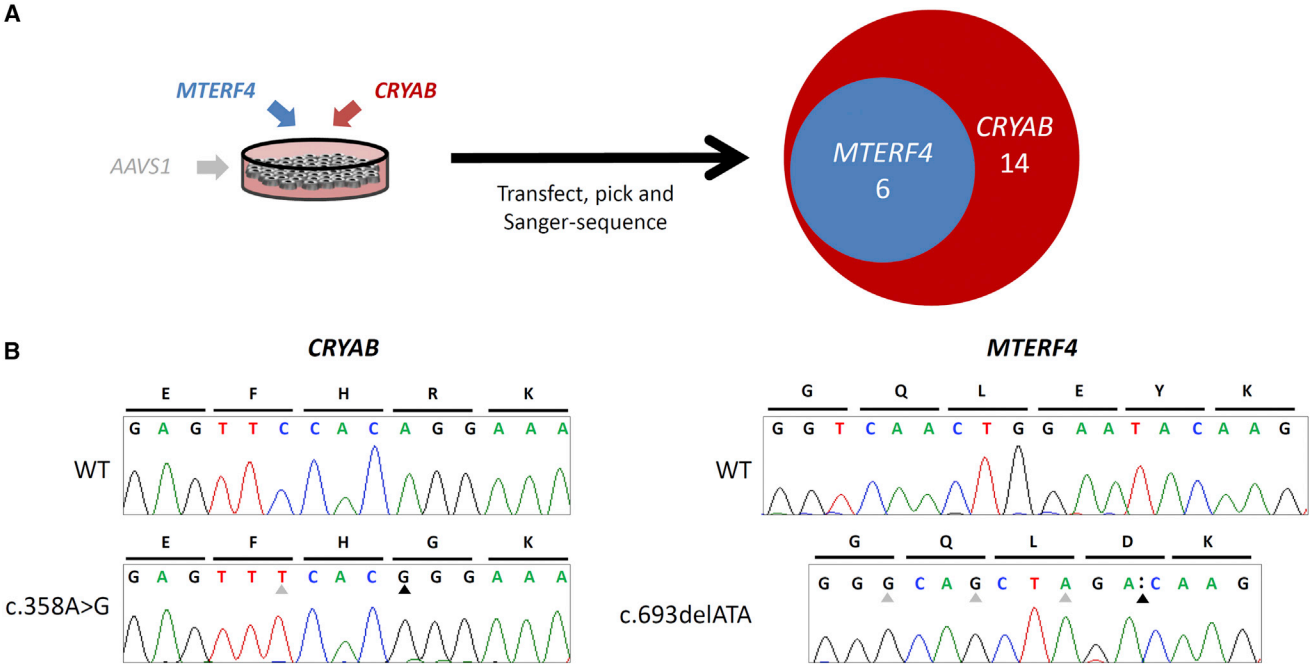

C

Clone	MTERF	CRYAB	Clone	MTERF	CRYAB	Clone	MTERF	CRYAB	Clone	MTERF	CRYAB	Clone	MTERF	CRYAB
1	WT/WT	Indel/Indel	11	WT/WT	Indel/Indel	21	WT/WT	Indel/Indel	31	Indel/Indel	WT/Indel	41	WT/WT	WT/WT
2	WT/WT	WT/WT	12	WT/Indel	KI/KI	22	WT/Indel	KI/KI	32	KI/Indel	KI/Indel	42	KI/Indel	KI/KI
3	WT/WT	WT/WT	13	WT/WT	WT/WT	23	KI/Indel	KI/KI	33	WT/WT	WT/WT	43	KI/Indel	KI/KI
4	WT/WT	WT/WT	14	WT/WT	KI/KI	24	Indel/Indel	KI/Indel	34	WT/WT	Indel/Indel	44	WT/Indel	Indel/Indel
5	WT/WT	WT/WT	15	WT/WT	WT/WT	25	WT/WT	WT/WT	35	WT/WT	WT/WT	45	WT/WT	WT/WT
6	WT/WT	WT/WT	16	WT/Indel	KI/KI	26	WT/Indel	Indel/Indel	36	WT/WT	KI/KI	46	WT/WT	WT/WT
7	WT/WT	KI/KI	17	WT/WT	WT/WT	27	WT/WT	WT/WT	37	WT/WT	WT/KI	47	KI/Indel	KI/KI
8	WT/WT	WT/WT	18	WT/WT	WT/WT	28	KI/Indel	KI/KI	38	WT/WT	WT/WT	48	WT/Indel	WT/WT
9	WT/WT	WT/Indel	19	WT/WT	Indel/Indel	29	WT/WT	WT/WT	39	WT/WT	Indel/Indel	49	WT/WT	WT/WT
10	WT/WT	WT/WT	20	WT/WT	Indel/Indel	30	WT/WT	WT/WT	40	WT/WT	WT/WT	50	Indel/Indel	Indel/Indel

Figure 4. Simultaneous Dual Modification using CTS

(A) Dual modification was attempted on hB53 hiPS6 using components for targeting *MTERF4*:c.693delATA and *CRYAB*:c.358A>G. Following CTS, 50 clones were sequenced and, of those, 14 had knockin at *CRYAB* (depicted in the red circle) and 6 had knockin at *MTERF4* (depicted in the blue circle). All 6 of the cells with *MTERF4* knockin also had knockin at *CRYAB*. Given individual editing rates, the likelihood of co-occurrence assuming random distribution of events is 5%. We observed a disproportionate co-occurrence of dual modification with a FET < 0.001.

(B) Representative chromatograms of dual-targeted clones at each loci and WT sequence. Black arrows indicate variant of interest position. Silent, engineered blocking mutations that prevent re-targeting by Cas9 are indicated by gray arrows.

(C) Table including genotypes of individual clones at both (*MTERF4* and *CRYAB*) loci. WT, unmodified; KI, knockin; Indel, insertion or deletion. See also Table S3.

of complex diseases and especially the role of modifier loci, we envisage CTS being of potential utility for simultaneous recapitulation of multiple candidate variants. Indeed, using CTS, we concurrently delivered editing reagents designed to incorporate passenger mutations at two different loci and isolated multiple clones bearing both edits (Figure 4). It will be interesting to determine whether application of CTS in conjunction with polycistronic sgRNA delivery systems (Cong et al., 2013) will permit highly parallelized HDR-based genome editing.

Operationally, CTS provides a marked improvement in the efficiency of isolating precision-modified iPSC lines compared with direct cloning-based methods, without extended hands-on time or a requirement for additional instrumentation. Following methodological refinements and legislating for effect range, we conservatively estimate that a single well-trained technician could generate ten precision-edited cell lines in 1 month. CTS is generalizable in that, while the system described uses antibiotic resistance as the selectable modification, alternative HDR-based

reporters (e.g., insertion of a GFP cassette) could theoretically be employed. In our experiments, half of the analyzed clones were correctly targeted at AAVS1 with no additional random integration events, consistent with data reported previously (Hockemeyer et al., 2011), and this would likely be further improved with a gene trap approach. The site of the selectable modification could also be adapted depending on context and user requirements. For example, knockin of a GFP tag into a cardiac transcription factor such as NKX2-5 (Elliott et al., 2011) would yield iPSCs that harbor a variant of interest in tandem with a reporter which assists cardiomyocyte isolation. Furthermore, compared with alternative knockin strategies facilitated by targeted insertion of a selectable marker, CTS does not require the production of gene-specific custom targeting vectors, making it a readily scalable strategy. In addition, while we observed no adverse effects of *AAVS1* targeting or carriage of the *pac* cassette on cell behavior or differentiation potential (although appropriate isogenic control cell lines harboring only the *pac* cassette should be utilized for phenotypic evaluation), removal of the *pac* cassette could be performed through transfection of cells with *piggyBac* transposase, although excision/re-integration rates would need to be empirically determined. Removal of the *pac* cassette would be required for any subsequent modification of generated cell lines with the same CTS strategy. Finally, a detailed mechanistic examination of the processes (e.g., engagement of HDR proteins, chromatin reorganization) that distinguish *HDR-responsive* from *HDR-refractory* cells and which contribute to the reported observations will be necessary and will undoubtedly catalyze discovery of additional factors which augment precision genome editing in all cell systems.

EXPERIMENTAL PROCEDURES

Detailed Experimental Procedures are available in the Supplemental Information.

Targeting Reagents

CRISPR target sites proximal to the SNP of interest were identified using ZiFiT Targeter Version 4.2 and were cloned into pX330-U6-Chimeric_BB-CBh-hSpCas9 (a gift from Feng Zhang, Addgene plasmid no. 42230) as described previously (Cong et al., 2013). Cleavage efficacy of designed vectors was validated using the Cel-1 Surveyor assay as described previously (Geurts et al., 2009; Miller et al., 2007). Cognate, variant-specific ssODNs were designed and include silent mutations to prevent re-cutting of Cas9 following HDR. The *AAVS1* Safe Harbor TALE-Nuclease Kit was purchased from System Biosciences, including p*AAVS1* Dual Promoter Donor Vector (GE602A-1) and the TALE-Nuclease Vectors, pZT-*AAVS1* L1 TALE-N Vector (GE601A-1) and pZT-*AAVS1* R1 TALE-N Vector (GE601A-1) previously shown to have minimal off-target cleavage (Hockemeyer et al., 2011). A second *AAVS1* Safe Harbor Kit was purchased from Transposagen, the Puro-TK with XTN TALEN (catalog no. KSH-004).

iPSC Lines and Culture

All human subject research was approved by the Medical College of Wisconsin and University of Utah institutional review boards. The human iPSC lines used in this study are hB53 hiPS6 (Riedel et al., 2014) and hB119 hiPS9, derived as described previously (Riedel et al., 2014). Informed consent was obtained for this procedure. iPSCs were cultured as described previously (Mitzelfelt et al., 2016).

iPSC Transfection

Transfection of relevant components was performed in iPSCs using a 4D-Nucleofector (Lonza). Following transfection, cells underwent the CTS protocol outlined in Figure S1 and detailed in the Supplemental Experimental Procedures. For deep-sequencing analysis of pooled populations (Figure 2), iPSCs were transfected and cultured as described, except that 2-day post transfection cells were separated into two groups, –CTS and +CTS, with corresponding –CTS and +CTS samples derived from the same initial transfection. +CTS conditions were as shown in Figure S1; –CTS conditions were identical, except that puromycin was omitted. Cells were pooled and genomic DNA was analyzed as described below.

Genotyping PCR and Sanger Sequencing for Clones

Genomic DNA was isolated and PCR was carried out using gene-specific primers. Resulting amplicons were Sanger sequenced using amplification primers.

Illumina MiSeq Library Preparation

Genomic DNA was isolated from pooled populations and samples were prepared and analyzed with the Illumina MiSeq, as described previously (Kistler et al., 2015).

Illumina MiSeq Analysis Methods

Reads were quality filtered using Trimmomatic (Bolger et al., 2014). Sorted/indexed BAM files were aligned to reference sequences (obtained from Ensembl release 84) with Bowtie2. Extent of HDR-mediated donor integration was quantified by interrogating FASTQ files for informative segments of the donor sequence (typically ~50 nucleotides, spanning the targeted nucleotide and CRISPR cut site) via in-house code, manual inspection, and third-party software.

PCR-Based Analysis of Integration of the *AAVS1* Donor Vector

HDR was confirmed at the *AAVS1* locus using inside-out PCR with one primer falling inside the exogenous sequence and one primer outside the homology arm (Figure S4B).

Immunocytochemistry and Karyotyping

Immunocytochemistry and karyotyping were performed as described previously (Mitzelfelt et al., 2016).

SUPPLEMENTAL INFORMATION

Supplemental Information includes Supplemental Experimental Procedures, four figures and three tables and can be found with this article online at http://dx.doi.org/10.1016/j.stemcr.2017.01.021.

AUTHOR CONTRIBUTIONS

Conceptualization, A.M.G., K.A.M., and C.M.D.R.; Methodology, A.M.G., K.A.M., and C.M.D.R.; Software and Formal Analysis, C.M.D.R.; Investigation, K.A.M., C.M.D.R., M.N.G., M.M., C.T.K., M.J.C., K.D.K., M.R., and S.L.; Resources, D.P.D., D.H., C.J.J., and M.T.F.; Writing – Original Draft, C.M.D.R.; Writing – Review & Editing, C.M.D.R., K.A.M., A.M.G., and I.J.B.; Visualization, C.M.D.R. and K.A.M.; Supervision, A.M.G., C.M.D.R., and K.A.M.; Funding Acquisition, A.M.G., I.J.B., K.A.M., C.M.D.R., and J.W.V.

ACKNOWLEDGMENTS

We thank Shirng-Wern Tsaih and Michael Tschannen (Human Molecular Genetics Center, Medical College of Wisconsin) for advice and technical support. This work was supported by NIH New Innovator Award 1DP2OD008396 (A.M.G.) and NIH Director's Pioneer Award Grant 8DP1HL17650-04 (I.J.B.), the Steven Cullen Healthy Heart Award (A.M.G.), made possible by the Research and Education Program Fund, a component of the Advancing a Healthier Wisconsin endowment at the Medical College of Wisconsin, a W.M. Keck Foundation Medical Research Grant (J.W.V.), and a Ruth L. Kirschstein National Research Service Award F31 Individual Fellowship 1F31AR067618-01A1 (K.A.M.).

Received: August 11, 2016
Revised: January 21, 2017
Accepted: January 21, 2017
Published: February 23, 2017

REFERENCES

Arribere, J.A., Bell, R.T., Fu, B.X.H., Artiles, K.L., Hartman, P.S., and Fire, A.Z. (2014). Efficient marker-free recovery of custom genetic modifications with CRISPR/Cas9 in *Caenorhabditis elegans*. Genetics *198*, 837–846.

Bhaya, D., Davison, M., and Barrangou, R. (2011). CRISPR-Cas systems in bacteria and archaea: versatile small RNAs for adaptive defense and regulation. Annu. Rev. Genet. *45*, 273–297.

Bolger, A.M., Lohse, M., and Usadel, B. (2014). Trimmomatic: a flexible trimmer for Illumina sequence data. Bioinformatics *30*, 2114–2120.

Cong, L., Ran, F.A., Cox, D., Lin, S., Barretto, R., Habib, N., Hsu, P.D., Wu, X., Jiang, W., Marraffini, L.A., et al. (2013). Multiplex genome engineering using CRISPR/Cas systems. Science *339*, 819–823.

Ding, Q., Lee, Y.-K., Schaefer, E.A.K., Peters, D.T., Veres, A., Kim, K., Kuperwasser, N., Motola, D.L., Meissner, T.B., Hendriks, W.T., et al. (2013a). A TALEN genome-editing system for generating human stem cell-based disease models. Cell Stem Cell *12*, 238–251.

Ding, Q., Regan, S.N., Xia, Y., Oostrom, L.A., Cowan, C.A., and Musunuru, K. (2013b). Enhanced efficiency of human pluripotent stem cell genome editing through replacing TALENs with CRISPRs. Cell Stem Cell *12*, 393–394.

Doench, J.G., Fusi, N., Sullender, M., Hegde, M., Vaimberg, E.W., Donovan, K.F., Smith, I., Tothova, Z., Wilen, C., Orchard, R., et al. (2016). Optimized sgRNA design to maximize activity and minimize off-target effects of CRISPR-Cas9. Nat. Biotech. *34*, 184–191.

Elliott, D.A., Braam, S.R., Koutsis, K., Ng, E.S., Jenny, R., Lagerqvist, E.L., Biben, C., Hatzistavrou, T., Hirst, C.E., Yu, Q.C., et al. (2011). NKX2-5eGFP/w hESCs for isolation of human cardiac progenitors and cardiomyocytes. Nat. Methods *8*, 1037–1040.

Flemr, M., and Buhler, M. (2015). Single-step generation of conditional knockout mouse embryonic stem cells. Cell Rep. *12*, 709–716.

Geurts, A.M., Cost, G.J., Freyvert, Y., Zeitler, B., Miller, J.C., Choi, V.M., Jenkins, S.S., Wood, A., Cui, X., Meng, X., et al. (2009). Knockout rats via embryo microinjection of zinc-finger nucleases. Science *325*, 433.

Gonzalez, F., Zhu, Z., Shi, Z.D., Lelli, K., Verma, N., Li, Q.V., and Huangfu, D. (2014). An iCRISPR platform for rapid, multiplexable, and inducible genome editing in human pluripotent stem cells. Cell Stem Cell *15*, 215–226.

Gutschner, T., Haemmerle, M., Genovese, G., Draetta, Giulio F., and Chin, L. (2016). Post-translational regulation of Cas9 during G1 enhances homology-directed repair. Cell Rep. *14*, 1555–1566.

Hockemeyer, D., and Jaenisch, R. (2016). Induced pluripotent stem cells meet genome editing. Cell Stem Cell *18*, 573–586.

Hockemeyer, D., Wang, H., Kiani, S., Lai, C.S., Gao, Q., Cassady, J.P., Cost, G.J., Zhang, L., Santiago, Y., Miller, J.C., et al. (2011). Genetic engineering of human pluripotent cells using TALE nucleases. Nat. Biotechnol. *29*, 731–734.

Kistler, K.E., Vosshall, L.B., and Matthews, B.J. (2015). Genome engineering with CRISPR-Cas9 in the mosquito Aedes aegypti. Cell Rep. *11*, 51–60.

Liao, S., Tammaro, M., and Yan, H. (2015). Enriching CRISPR-Cas9 targeted cells by co-targeting the HPRT gene. Nucleic Acids Res. *43*, e134.

Lin, S., Staahl, B.T., Alla, R.K., and Doudna, J.A. (2014). Enhanced homology-directed human genome engineering by controlled timing of CRISPR/Cas9 delivery. Elife *3*, e04766.

Long, C., McAnally, J.R., Shelton, J.M., Mireault, A.A., Bassel-Duby, R., and Olson, E.N. (2014). Prevention of muscular dystrophy in mice by CRISPR/Cas9–mediated editing of germline DNA. Science *345*, 1184–1188.

Maruyama, T., Dougan, S.K., Truttmann, M.C., Bilate, A.M., Ingram, J.R., and Ploegh, H.L. (2015). Increasing the efficiency of precise genome editing with CRISPR-Cas9 by inhibition of nonhomologous end joining. Nat. Biotech. *33*, 538–542.

Miller, J.C., Holmes, M.C., Wang, J., Guschin, D.Y., Lee, Y.-L., Rupniewski, I., Beausejour, C.M., Waite, A.J., Wang, N.S., Kim, K.A., et al. (2007). An improved zinc-finger nuclease architecture for highly specific genome editing. Nat. Biotech. *25*, 778–785.

Mitzelfelt, K.A., Limphong, P., Choi, M.J., Kondrat, F.D., Lai, S., Kolander, K.D., Kwok, W.M., Dai, Q., Grzybowski, M.N., Zhang, H., et al. (2016). Human 343delT HSPB5 chaperone associated with early-onset skeletal myopathy causes defects in protein solubility. J. Biol. Chem. *291*, 14939–14953.

Miyaoka, Y., Chan, A.H., Judge, L.M., Yoo, J., Huang, M., Nguyen, T.D., Lizarraga, P.P., So, P.-L., and Conklin, B.R. (2014). Isolation of single-base genome-edited human iPS cells without antibiotic selection. Nat. Methods *11*, 291–293.

Moriarity, B.S., Rahrmann, E.P., Beckmann, D.A., Conboy, C.B., Watson, A.L., Carlson, D.F., Olson, E.R., Hyland, K.A., Fahrenkrug, S.C., McIvor, R.S., et al. (2014). Simple and efficient methods for enrichment and isolation of endonuclease modified cells. PLoS One *9*, e96114.

Paquet, D., Kwart, D., Chen, A., Sproul, A., Jacob, S., Teo, S., Olsen, K.M., Gregg, A., Noggle, S., and Tessier-Lavigne, M. (2016). Efficient introduction of specific homozygous and heterozygous mutations using CRISPR/Cas9. Nature *533*, 125–129.

Riedel, M., Jou, C.J., Lai, S., Lux, R.L., Moreno, A.P., Spitzer, K.W., Christians, E., Tristani-Firouzi, M., and Benjamin, I.J. (2014). Functional and pharmacological analysis of cardiomyocytes differentiated from human peripheral blood mononuclear-derived pluripotent stem cells. Stem Cell Rep. *3*, 131–141.

Sadelain, M., Papapetrou, E.P., and Bushman, F.D. (2012). Safe harbours for the integration of new DNA in the human genome. Nat. Rev. Cancer *12*, 51–58.

Soldner, F., Laganière, J., Cheng, A.W., Hockemeyer, D., Gao, Q., Alagappan, R., Khurana, V., Golbe, L.I., Myers, R.H., Lindquist, S., et al. (2011). Generation of isogenic pluripotent stem cells differing exclusively at two early onset Parkinson point mutations. Cell *146*, 318–331.

Tsai, S.Q., Zheng, Z., Nguyen, N.T., Liebers, M., Topkar, V.V., Thapar, V., Wyvekens, N., Khayter, C., Iafrate, A.J., Le, L.P., et al. (2015). GUIDE-seq enables genome-wide profiling of off-target cleavage by CRISPR-Cas nucleases. Nat. Biotech. *33*, 187–197.

Wang, G., McCain, M.L., Yang, L., He, A., Pasqualini, F.S., Agarwal, A., Yuan, H., Jiang, D., Zhang, D., Zangi, L., et al. (2014). Modeling the mitochondrial cardiomyopathy of Barth syndrome with induced pluripotent stem cell and heart-on-chip technologies. Nat. Med. *20*, 616–623.

Ward, J.D. (2015). Rapid and precise engineering of the *Caenorhabditis elegans* genome with lethal mutation co-conversion and inactivation of NHEJ. Repair Genet. *199*, 363–377.

Yang, L., Guell, M., Byrne, S., Yang, J.L., De Los Angeles, A., Mali, P., Aach, J., Kim-Kiselak, C., Briggs, A.W., Rios, X., et al. (2013). Optimization of scarless human stem cell genome editing. Nucleic Acids Res. *41*, 9049–9061.

Yu, C., Liu, Y., Ma, T., Liu, K., Xu, S., Zhang, Y., Liu, H., La Russa, M., Xie, M., Ding, S., et al. (2015). Small molecules enhance CRISPR genome editing in pluripotent stem cells. Cell Stem Cell *16*, 142–147.

Yusa, K., Rashid, S.T., Strick-Marchand, H., Varela, I., Liu, P.-Q., Paschon, D.E., Miranda, E., Ordonez, A., Hannan, N.R.F., Rouhani, F.J., et al. (2011). Targeted gene correction of [agr]1-antitrypsin deficiency in induced pluripotent stem cells. Nature *478*, 391–394.

Stem Cell Reports, Volume *8*

Supplemental Information

Efficient Precision Genome Editing in iPSCs via Genetic Co-targeting with Selection

Katie A. Mitzelfelt, Chris McDermott-Roe, Michael N. Grzybowski, Maribel Marquez, Chieh-Ti Kuo, Michael Riedel, Shuping Lai, Melinda J. Choi, Kurt D. Kolander, Daniel Helbling, David P. Dimmock, Michele A. Battle, Chuanchau J. Jou, Martin Tristani-Firouzi, James W. Verbsky, Ivor J. Benjamin, and Aron M. Geurts

Supplemental Information

Supplemental Figures

Figure S1: Timeline for CTS protocol. Related to Figure 1.

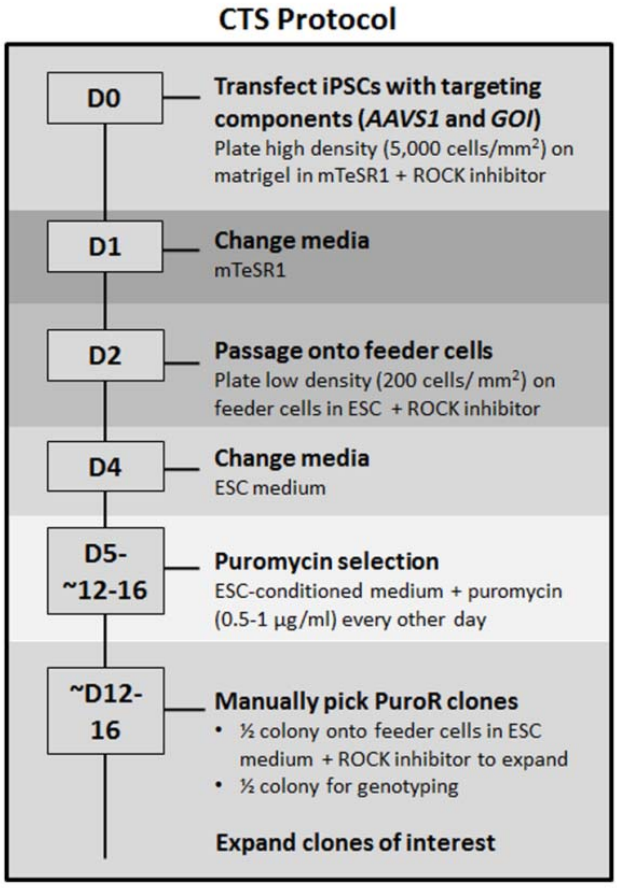

iPSCs are transfected with targeting components shown in Figure 1a on day 0 (D0) and plated at high density on matrigel to promote survival in mTeSR1 medium supplemented with ROCK inhibitor. On D1, media is changed to fresh mTeSR1 and dead cells are washed away. Cells are passaged on D2 to mitomycin-C-treated SNL feeders cells at low density. Puromycin selection (0.5 µg/ml) is performed D5-picking time (~D12-16) in order to limit selection based on transient expression of puromycin resistance and promote selection for incorporation of the puromycin cassette into the *AAVS1* locus. Selection is continued until picking to ensure all cells picked are puromycin resistant. Colonies are manually picked ~D12-16, with half of the colony utilized for genotyping while the other half is re-plated for expansion.

Figure S2: Experimental design comparing selection methods. Related to Figure 1.

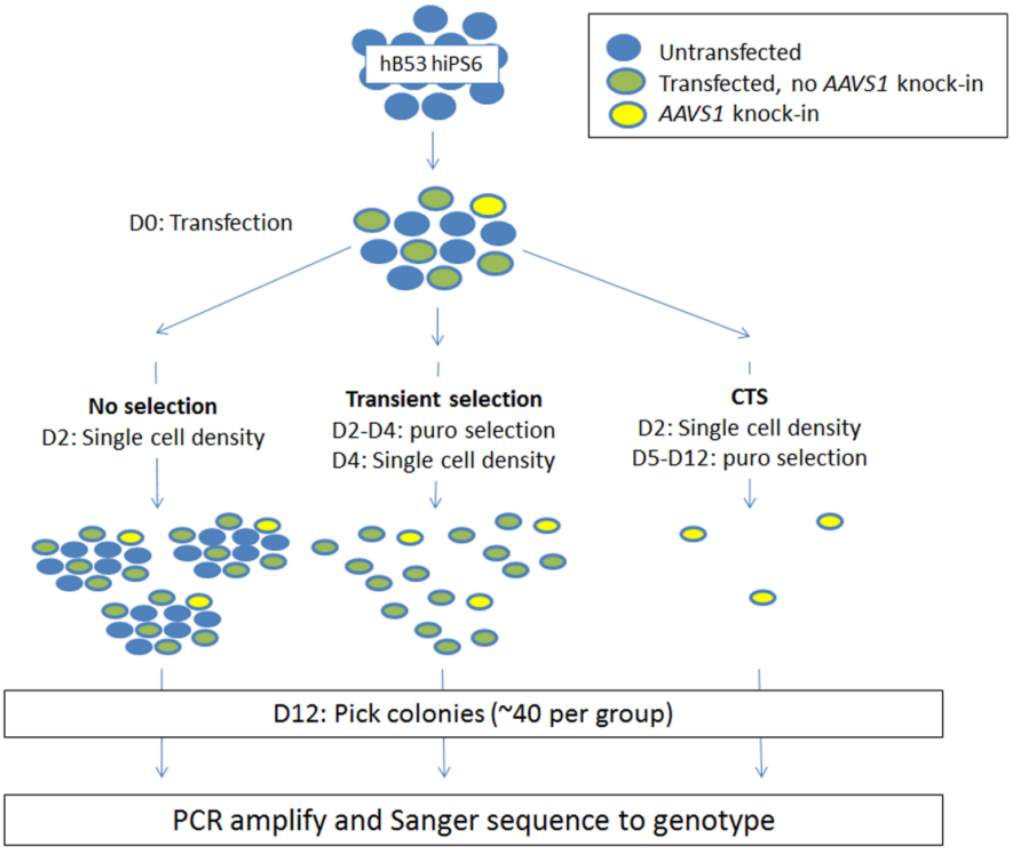

Experimental design employed for comparing selection strategies (no selection, transient selection, and CTS) used for generating data shown in Table S1 and Figure 1c.

Figure S3: Concordance between deep-sequencing pooled samples and direct sequencing clonal samples. Related to Figure 2-3 and Table S2-S3.

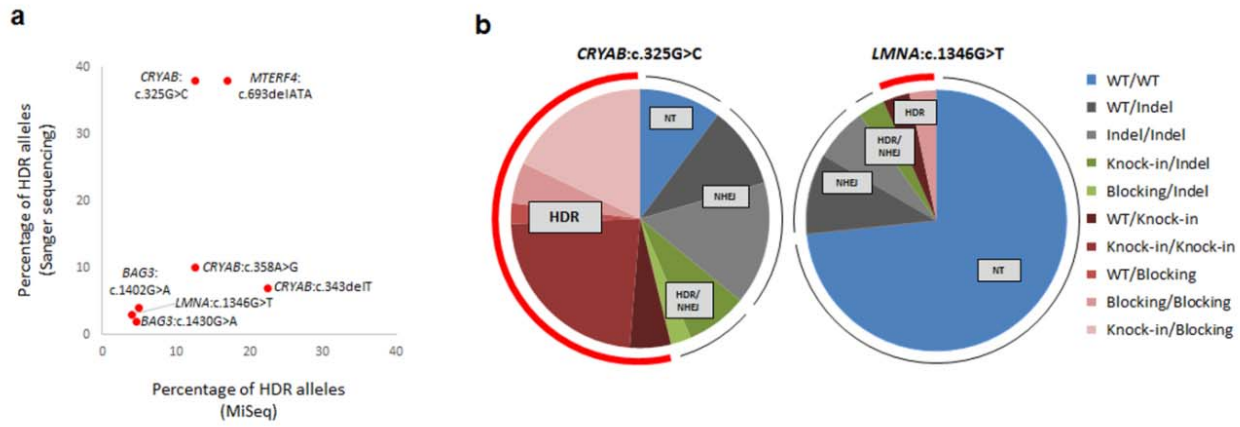

(a) Correlation of allelic HDR frequency between deep-sequencing (MiSeq) of pooled populations and Sanger sequencing of clonal populations. (b) Representative examples of high (CRYAB:c.325G>C) and low (LMNA:c.1346G>T) efficiency loci showing genotypes derived from clonally expanded populations. 'Blocking' indicates knock-in of only the silent, Cas9-blocking mutation (i.e., without the variant of interest), whereas 'Knock-in' indicates incorporation of both the silent mutation and variant of interest. 'WT' indicates unmodified alleles. Genotypes are categorized as not-targeted (NT), NHEJ, HDR and NHEJ (HDR/NHEJ), or HDR.

Figure S4: Knock-in and random integration at *AAVS1*. Related to Figures 1 and 3.
(a) Schematics of commercially available targeting vectors used in experiments from System Biosciences (SBI) and Transposagen. Abbreviations: HA, homology arm; PGK, phosphoglycerate kinase promoter; MCS, multiple cloning site; EF1α, elongation factor 1 α promoter; GFP, green fluorescent protein; T2A, self-cleaving peptide sequence; Puro, puromycin resistance gene (*pac*); TR, *piggyBac* terminal repeats; TK, thymidine kinase. Relative locations of PCR Primers used for random integration and internal control primers are shown. (b) Schematic representation of HDR-mediated integration at the *AAVS1* locus. Relative positions of Southern blotting probe (red block), double strand break (DSB), exons (E), EcoRV cut sites, and inside-out PCR primers (SBI 5' F/R and SBI 3' F/R) are shown. Expected sizes for targeted (2.9 kb) and untargeted (5.4 kb) fragments by Southern blot are shown. (c) Forty-eight clones derived from transfection of the AAVS1 donor vector and TALEN constructs following the CTS protocol (Figure S1) were screened by Southern blotting and a PCR-based integration assay for knock-in at *AAVS1*. For Southern blotting, genomic DNA was digested with EcoRV and hybridized with a ^{32}P-labeled probe recognizing the 5' homology arm (shown in b). A 5.4 kb untargeted or wildtype (WT) band and a 2.9 kb targeted or knock-in (KI) band is observed. Additional bands observed are predicted to be random integration events of the donor vector elsewhere in the genome. PCR was performed using inside-out primers (demonstrating targeted integration), random primers (specific for the vector backbone), and internal primers (integration control) (primer sequences and fragment sizes are shown in Supplemental Experimental Procedures) and run on agarose gels. Clones with targeted knock-in (either heterozygous or homozygous) and without additional random integration events are indicated with asterisk (*). Genomic DNA used in the final column was from untargeted (WT) cells as a control.

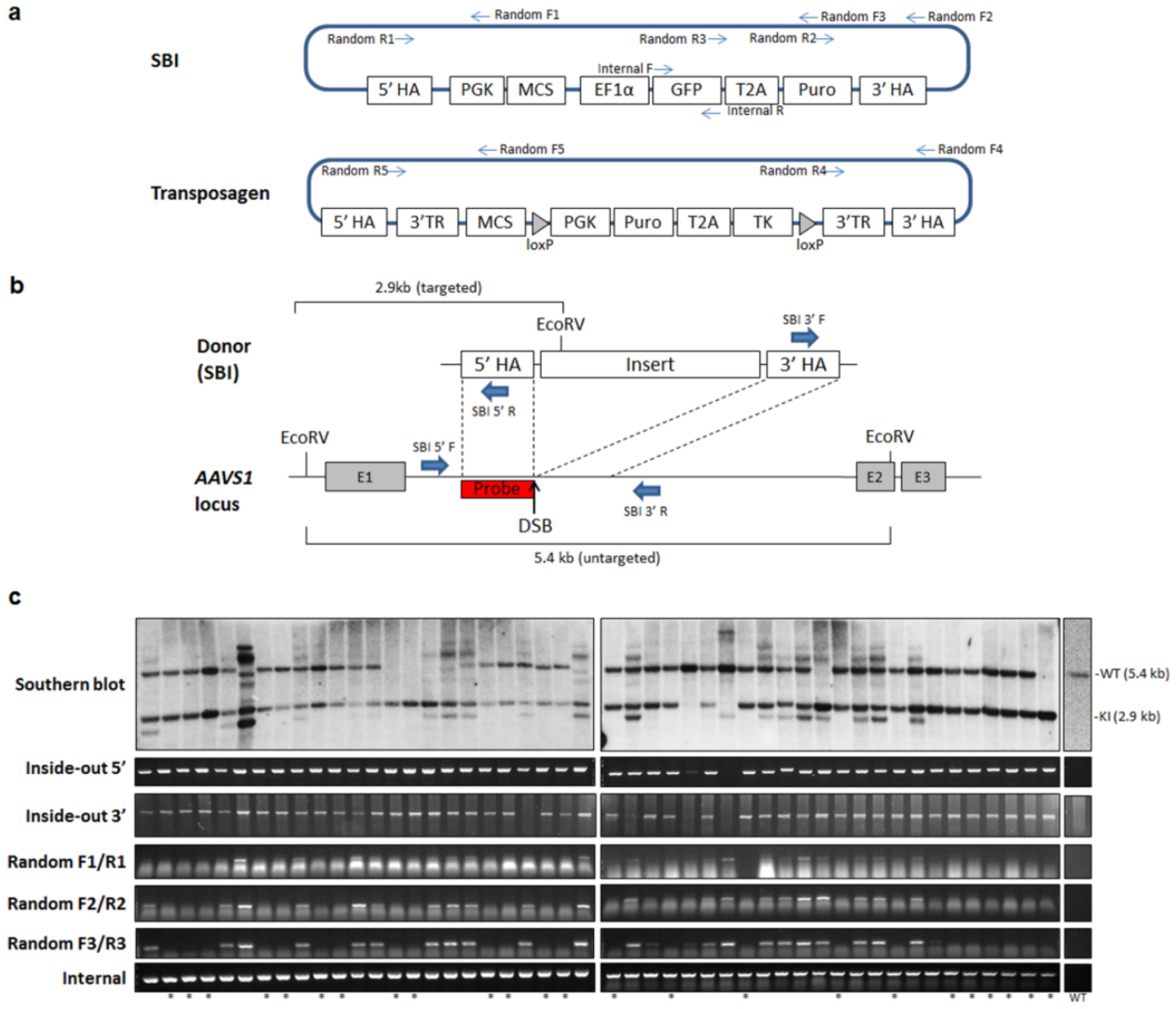

Supplemental Tables

Table S1: Genotypes of clones analyzed comparing different selection strategies. Related to Figure 1.

Selection	None	Transient	CTS
WT/WT	39	43	4
WT/Indel	3	1	4
Indel/Indel	1	1	6
Knock-in/Indel	1	2	3
Blocking/Indel	0	0	1
WT/Knock-in	0	0	2
Knock-in/Knock-in[#]	0	1	9
WT/Blocking	1	0	1
Blocking/Blocking[#]	0	0	2
Knock-in/Blocking	1	0	7
Total	46	48	39

Genotypes of clones analyzed by direct Sanger sequencing of PCR products (presented in Figure 1c). 'Blocking' indicates knock-in of only the silent, Cas9-blocking mutation (i.e., without the variant of interest), whereas 'Knock-in' indicates incorporation of both the silent mutation and variant of interest. 'WT' indicates unmodified alleles. CTS column from this table is the same data shown in Table S3.

[#]Though these clones appear to be homozygous through Sanger sequencing (i.e. 'clean' sequence), a Southern blot would be required prior to phenotyping to ensure there is not a large deletion on one allele that prevents PCR amplification.

Table S2: MiSeq experimental results. Related to Figure 2.

hB53 hiPS6	Total # reads	Total # edits	HDR		NHEJ		WT	
Sample			**# reads**	**% of total**	**# reads**	**% of total**	**# reads**	**% of total**
CRYAB:c.343delT_CTS-	262144	152720	**2458**	***1***	150262	*57*	109424	*42*
CRYAB:c.343delT_CTS+	134752	134752	**30210**	***22***	86683	*64*	17859	*13*
CRYAB:c.325G>C_CTS-	264167	168170	**2967**	***1***	165437	*63*	95997	*36*
CRYAB:c.325G>C_CTS+	135680	123981	**17227**	***13***	106754	*79*	11699	*9*
CRYAB:c.358A>G_CTS-	233189	129405	**2568**	***1***	126837	*54*	103784	*45*
CRYAB:c.358A>G_CTS+	299329	282460	**37946**	***13***	244515	*82*	16869	*6*
BAG3:c.1430G>A_CTS-	155400	13104	**439**	***0***	12665	*8*	142296	*92*
BAG3:c.1430G>A_CTS+	183997	61279	**8526**	***5***	52753	*29*	122718	*67*
BAG3:c.1402G>A_CTS-	180651	14651	**108**	***0***	14543	*8*	166000	*92*
BAG3:c.1402G>A_CTS+	160393	50311	**8042**	***5***	42269	*26*	110082	*69*
LMNA:c.1346G>T_CTS-	207467	9211	**20**	***0***	9191	*4*	198256	*96*
LMNA:c.1346G>T_CTS+	202658	25455	**2410**	***1***	23045	*11*	177203	*87*
MTERF4:c.693delATA_CTS-	188846	9255	**353**	***0***	8902	*5*	179591	*95*
MTERF4:c.693delATA_CTS+	174497	90735	**29916**	***17***	60819	*35*	83762	*48*
Average_CTS-	**213123**	**70931**	**1273**	**0.4**	**69691**	**28.4**	**142193**	**71.1**
Average_CTS+	**184472**	**109853**	**19182**	**10.9**	**88120**	**46.6**	**77170**	**42.7**

hB119 hiPS9	Total # reads	Total # edits	HDR		NHEJ		WT	
Sample			**# reads**	**% of total**	**# reads**	**% of total**	**# reads**	**% of total**
CRYAB:c.343delT_CTS-	121572	23748	**3108**	***3***	20640	*17*	97824	*80*
CRYAB:c.343delT_CTS+	110499	108887	**27905**	***25***	80982	*73*	1612	*1*
CRYAB:c.325G>C_CTS-	118811	69039	**774**	***1***	68265	*57*	49772	*42*
CRYAB:c.325G>C_CTS+	109238	75900	**9260**	***8***	66640	*61*	33338	*31*
CRYAB:c.358A>G_CTS-	100932	16806	**2447**	***2***	14359	*14*	84126	*83*
CRYAB:c.358A>G_CTS+	77869	75359	**41505**	***53***	33854	*43*	2510	*3*
BAG3:c.1430G>A_CTS-	91759	7878	**139**	***<1***	7739	*8*	83881	*91*
BAG3:c.1430G>A_CTS+	98513	21496	**10510**	***11***	10986	*11*	77017	*78*
BAG3:c.1402G>A_CTS-	95556	6920	**37**	***<1***	6883	*7*	88636	*93*
BAG3:c.1402G>A_CTS+	207563	45135	**11727**	***6***	33408	*16*	162428	*78*
LMNA:c.1346G>T_CTS-	112816	5463	**48**	***0***	5415	*5*	107623	*95*
LMNA:c.1346G>T_CTS+	220533	42597	8521	***4***	34436	*16*	177576	*81*
MTERF4:c.693delATA_CTS-	130614	9997	**1087**	***1***	8910	*7*	120617	*92*
MTERF4:c.693delATA_CTS+	93752	11555	**8111**	***9***	3444	*4*	82197	*88*
Average_CTS-	**110294**	**19979**	**1091**	**1.4**	**18887**	**16.4**	**90354**	**82.3**
Average_CTS+	**131138**	**54418**	**16791**	**16.6**	**37679**	**32.0**	**76668**	**51.4**

MiSeq experimental results for each cell line (hB53 hiPS6- top and hB119 hiPS9- bottom) including total number of reads, total number of edits, number of reads with HDR, percent of reads with HDR, number of reads with NHEJ, percent of reads with NHEJ, number of WT (unmodified) reads, and percent WT reads. Data for each variant with (CTS+) and without (CTS-) CTS are shown in individual rows with the final two rows showing average values including all variants. Each row indicates a single editing experiment.

Table S3: Information regarding generation of knock-in cell lines. Related to Figure 2-4.

	Gene	*Crystallin, Alpha B or HSPB5 (CRYAB)*			*BCL2-Associated Athanogene 3 (BAG3)*		*Lamin A/C (LMNA)*	*Mitochondrial Transcription Termination Factor 4 (MTERF4)*
Variant Information	Location	11q23.1			10q25.2-q26.2		1q22	2q37.3
	Mutation	c.343delT	c.325G>C	c.358A>G	c.1430G>A	c.1402G>A	c.1346G>T	c.[693delATA]; [787C>T] *
	Protein change	p.S115Pfs*14	p.D109H	p.R120G	p.R477H	p.V468M	p.G449V	p.[E231D,Y232del]; [Q263*]
	Disease	skeletal myopathy	cardiomyopathy, skeletal myopathy, cataracts	cardiomyopathy, skeletal myopathy, cataracts	dilated cardiomyopathy	dilated cardiomyopathy	muscular atrophy	hypertrophic cardiomyopathy
	Reference	(Forrest et al., 2011)	(Sacconi et al., 2012)	(Vicart et al., 1998)	(Norton et al., 2011)	(Villard et al., 2011)	(Dialynas et al., 2012)	Unpublished data
Targeting Information	AAVS1 Targeting Vector	Transposagen	SBI	Transposagen	SBI	SBI	Transposagen	SBI
	sgRNA/ssODN Orientation	R+	R+	R+	R-	R-	R+	R-
	Cell Line	hB53 hiPS6	hB53 hiPS6	hB53 hiPS6	hB53 hiPS6	hB53 hiPS6	hB119 hiPS9	hB53 hiPS6
Genotype	Unmodified	9	4	13	61	75	22	13
	WT/Indel	0	4	0	2	7	3	0
	Indel/Indel	4	6	5	0	2	2	2
	Knock-in/indel	0	3	0	1	1	1	4
	Blocking/Indel	0	1	0	0	1	0	0
	WT/Knock-in	0	2	0	1	3	1	0
	Knock-in/Knock-in#	1	9	2	0	1	0	11
	WT/Blocking	0	1	0	0	0	0	0
	Blocking/Blocking#	0	2	0	0	0	1	0
	Knock-in/Blocking	0	7	0	0	1	0	0
	Total	14	39	20	65	91	30	30

Variants of interest knocked-in to iPSCs using CTS. Gene name, mutation, corresponding protein change, disease, and references are given for each variant. The *AAVS1* targeting vector utilized in each case is shown (see Experimental Procedures). The sgRNA/ssODN orientation is listed as either R+ or R-, indicating agreement or disagreement with the Richardson et al. model for ssODN strand design (Richardson et al., 2016). The cell line utilized to generate each variant is also listed (hB53 hiPS6 or hB119 hiPS9). The numbers of clones isolated with each genotype are indicated below each variant and are derived from one experiment per variant. *The patient variant *MTERF4*:c.[693delATA];[787C>T] was generated by an ssODN incorporating c.693delATA and screening for an indel on the second allele to mimic c.787C>T, which generates a stop codon. #Though these clones appear to be homozygous through Sanger sequencing (i.e. 'clean' sequence), a Southern blot would be required prior to phenotyping to ensure there is not a large deletion on one allele that prevents PCR amplification.

Supplemental Experimental Procedures

CRISPR target site design and plasmid construction

CRISPR target sites proximal (within 35 bps) to the SNP of interest were identified using ZiFiT Targeter Version 4.2. Target sites as unique as possible – based on dissimilarity to other genomic loci - were selected and are shown in the table below. Typically, sites were chosen that had zero or one 'off by 0' or 'off by 1' matches elsewhere in the genome. pX330-U6-Chimeric_BB-CBh-hSpCas9 was a gift from Feng Zhang (Addgene plasmid # 42230). Reverse complementary oligonucleotide pairs with BbsI overhangs were purchased from Sigma (or Life Technologies) and hybridized, and cloned into the pX330 vector as described previously (Cong et al., 2013).

Locus	Guide RNA complementarity regions (5'-3')	Cleavage efficiency (%)
CRYAB	GGGATCCGGTATTTCCTG ()	5.4
BAG3	GGGACGAGCCGATGTGCGTC	8.8
LMNA	CATTGGACTTGTTGCGCAGC	13.3
MTERF4	ACTTGTATTCCAGTTGACCC	4.8

Culture and transfection of HEK293T cells and Cel-1 surveyor assay

HEK293T cells, maintained in Dulbecco's modified Eagle medium (DMEM) with high glucose, sodium pyruvate and L-glutamine (Life Technologies) supplemented with 10% fetal bovine serum (FBS- Life Technologies) and 100 u penicillin/100ug streptomycin/ml media (P/S- Life Technologies), were passaged using 0.05% Trypsin (Life Technologies) for transfection. For validating cleavage efficiencies of designed CRISPR guides, HEK 293T cells were mixed with SF nucleofection solution (Lonza) and various pX330 plasmids and transfected with the 4D Nucleofector™ (Lonza) using program CM-130. Cells were harvested 48 hours later and CRISPR activity was validated using the Cel-1 Surveyor assay (cutting efficiencies displayed in last column of the above table) as previously described (Geurts et al., 2009; Miller et al., 2007).

ssODN design

We typically designed ssODNs to flank the variant and/or cut-site by approximately 60bp on either side. In keeping with previous reports (Chen et al., 2011; Long et al., 2014; Paquet et al., 2016; Ponce de León et al., 2014), silent mutations were incorporated into the ssODNs to prevent re-cutting by Cas9 following HDR. This was achieved either through disruption of the PAM sequence or multiple disruptions within the target sequence. ssODNs utilized in experiments are shown in the table below.

Variant	ssODN Sequence (5'-3')
CRYAB: c.343delT	TGTTCTTATCTCTCTGCCTCTTTCCTCATTCTTTTGGGTTAGGATGAACATGGTTTCATCCCAGG GAGTTCAACAGGAAATACCGGATCCCAGCTGATGTAGACCCTCTCACCATTACTTCATCCCTG TCATCTGA
CRYAB: c.325G>C	GCAGGTGATAATAGTTCCTGTTCTTATCTCTCTGCCTCTTTCCTCATTCTTTTGGGTTAGCATGA ACATGGTTTCATCTCCAGGGAGTTTCACAGGAAATACCGGATCCCAGCTGATGTAGACCCTCT CACCATTACTTCATCCCTGTCATCTGA
CRYAB: c.358A>G	GCCTCTTTCCTCATTCTTTTGGGTTAGGATGAACATGGTTTCATCTCCAGGGAGTTTCACGGGA AATACCGGATCCCAGCTGATGTAGACCCTCTCACCATTACTTCATCCCTGTCATCTGA
BAG3: c.1430G>A	CCTGATGATCGAAGAGTATTTGACCAAAGAGCTGCTGGCCCTGGATTCAGTGGACCCCGAGGG GCGGGCAGACGTCCATCAGGCCAGGAGAGACGGTGTCAGGAAGGTTCAGACCATCTTGGAAA AACTTGAACAGAAAG
BAG3: c.1402G>A	CCTGATGATCGAAGAGTATTTGACCAAAGAGCTGCTGGCCCTGGATTCAATGGACCCCGAGGG GCGGGCAGACGTCCGGCAGGCCAGGAGAGACGGTGTCAGGAAGGTTCAGACCATCTTGGAAA AACTTGAACAGAAAG
LMNA: c.1346G>T	ACGCACTAGCGGGCGCGTGGCCGTGGAGGAGGTGGATGAGGAGGGCAAGTTTGTACGGCTGC GCAACAAGTCCAATGAGgtaggctcctgctcagggtctaaggggatacagctgcatca
MTERF4: c.693delATA	ccagtcattctcacctgaaactacgctaatcacgctatcagtcattctcacCTGAAACTTGTCTAGCTGCCCCAGGTCCTCTCG AAGAACAGAGGGGCAACTGTGCAAAATCTTGGTGACTTGCTGTACCGTGAAAAGGCA

AAVS1 targeting plasmids

The *AAVS1* Safe Harbor TALE-Nuclease kit was purchased from System Biosciences (SBI), including TALENs previously shown to have minimal off-target cleavage (Hockemeyer et al., 2011). Plasmids include the HDR donor

vector (Figure S4a), p*AAVS1* Dual Promoter Donor Vector (GE602A-1) containing GFP-Puromycin resistance cassette driven by an *EF1α* promoter, and the TALE-Nuclease Vectors, pZT-*AAVS1* L1 TALE-N Vector (GE601A-1) and pZT-*AAVS1* R1 TALE-N Vector (GE601A-1). These were used for all Illumina MiSeq experiments (except hB119 hiPS9 *LMNA*:c.1346 G>T), and for clonal knockin of *BAG3*:c.1430G>A, *BAG3:*c.1402G>A, *MTERF4*:c.693delATA, and *CRYAB*:c.325G>C. A second *AAVS1* Safe-harbor kit was purchased from Transposagen (Puro-TK with XTN™ TALEN, Catalog # KSH-004) with the donor vector that includes a puromycin resistance gene and thymidine kinase selection cassette driven by a *PGK* promoter and flanked by *piggyBac* repeats (Figure S4a), which can be sequentially, seamlessly removed with excision by *piggyBac* transposase if desired, as well as the accompanying *AAVS1*-specific XTN Forward and Reverse TALEN nucleases. The Transposagen system was used for generating *CRYAB*:c.358A>G and *CRYAB*:c.343delT clones. Additionally, we designed and validated a sgRNA targeting the *AAVS1* locus (guide RNA complementarity region (5'-3') GTCACCAATCCTGTCCCTAG) cloned into pX330 as described above. This pX330-*AAVS1* was used in concert with the *AAVS1* donor vector from Transposagen for generating *LMNA*:c.1346G>T clones and for Illumina MiSeq analysis of hB119 hiPS9 *LMNA*:c.1346G>T.

iPSC lines

All human subject research was approved by the Medical College of Wisconsin and University of Utah Institutional Review Boards. The human iPSC lines used in this study are hB53 hiPS6 (Riedel et al., 2014), derived from a 25-year-old Caucasian male and hB119 hiPS9, derived from peripheral blood mononuclear cells of a healthy 34-year-old Caucasian male using a polycistronic lentivirus containing *OCT4*, *KLF4*, *SOX2*, and *c-MYC* as previously described (Riedel et al., 2014). Informed consent was obtained for this procedure. hB53 hiPS6 was used for generating cell lines with the following knock-in mutations: *BAG3*:c.1402G>A, *BAG3*:c.1430G>A, *MTERF4*:c.693delATA, *CRYAB*:c.358A>G, *CRYAB*:c.325G>C and *CRYAB*:c.343delT, as well as the dual targeting experiment. hB119 hiPS9 was used for generating the cell line containing *LMNA*:c.1346G>T. We successfully applied our CTS method to two other iPSC lines (data not shown): knocking-in *CRYAB*:c.358A>G and *CRYAB:*c.325G>C mutations into hB119 hips10 (an alternate iPSC line derived from the same individual as hB119 hiPS9 using the same method, unpublished data) and reverting homozygous *CRYAB:*c.343delT to homozygous wildtype in a female iPSC line derived from the patient (Forrest et al., 2011), which was reprogrammed using retrovirus (Mitzelfelt et al., 2016).

iPSC culture

Prior to transfection, iPSCs were cultured as previously described (Mitzelfelt et al., 2016) in feeder-free conditions on Matrigel (Corning)-coated 6-well plates with mTeSR1 (Stem Cell Technologies) or StemMACS iPS-Brew XF (Miltenyi Biotec). Cells were passaged every 3-4 days using Accutase (Life Technologies) and seeded in media containing 10μM Rho-associated, coiled-coil containing protein kinase (ROCK) inhibitor (Y-27632, Selleck) for 24 hours following passaging.

iPSC Transfection

CTS for generation of knock-in iPSC lines– iPSCs were pretreated for 3-4 hours with 10μM ROCK inhibitor, washed once with Dulbecco's phosphate buffered saline (DPBS- Life Technologies), and incubated with Accutase (Life Technologies) for 5-8 minutes. Wash medium (Knockout DMEM/F12 supplemented with 10% FBS- both from Life Technologies) was added and cells were pipette vigorously to generate a single cell solution and counted using a Countess Automated Cell Counter (Life Technologies). For each transfection (*day 0*), 1μg of the gene-specific pX330 CRISPR/Cas9 plasmid, 2μl of a 40μM stock solution or 1.5μl of a 20μM stock solution of the relevant ssODN, 1μg of each of the two *AAVS1*-specific TALEN plasmids (or 1μg of the *AAVS1*-specific pX330 CRISPR plasmid) and 1μg *AAVS1* donor plasmid (see Targeting Reagents above) were added to 100μl P4 solution (Lonza) and electroporated using program CB-150 on a 4D Nucleofector™ into iPSCs ($1x10^6$ cells/transfection). Cells from each transfection were then seeded into one well of Matrigel-coated 24-well plate (5,000 cells/mm^2) for recovery in mTeSR1 or StemMACS iPS-Brew XF supplemented with 10μM ROCK inhibitor. The following day (*day 1*), cells were washed once with DPBS to remove dead cells and media was changed to mTeSR1 or StemMACS iPSC-Brew XF. Two days post-transfection (*day 2*), iPSCs were dispersed using Accutase and distributed across a 6-well plate pre-seeded with Mitomycin C (SantaCruz) -treated SNL feeder cells (Cell Biolabs) in ESC medium, composed of Knockout DMEM (Life Technologies) supplemented with 20% Knockout Serum Replacement (Life Technologies), MEM-NEAA (Life Technologies), 2mM L-glutamine (Life Technologies), P/S, 0.1mM β-mercaptoethanol (Sigma), 10ng/ml human basic fibroblast growth factor (bFGF, Cell Signaling), and 50ng/ml L-ascorbic acid (Sigma), supplemented with 10μM ROCK inhibitor. Media was changed two days later

(*day 4*) to ESC medium minus ROCK inhibitor. Three days post-seeding (*day 5*), puromycin (0.5-1µg/ml)-supplemented ESC-conditioned media (ESC media conditioned on SNL feeder cells with bFGF and vitamin C added post-conditioning) was added and replaced thereafter every 2 days until picking time (~7-10 days). Waiting until *day* 5 to begin puromycin selection limits the extent of selection for transient expression of puromycin resistance and selecting until picking ensures that all colonies picked have integration of the *pac* cassette. Following ~7-10 days of maintenance in puromycin-containing media (*day 12-16*), distinct colonies (~1mm diameter) were apparent and manually/mechanically transferred each to a single well of a 24-well plate pre-seeded with feeder cells in ESC media plus ROCK inhibitor. Half of each isolate was retained for expansion and half for DNA isolation to genotype. Following genotyping (see below), desired clones were passaged to single wells of 12-well matrigel-coated dishes in mTeSR1 plus ROCK inhibitor and further expanded for pluripotency immunocytochemistry and karyotyping (see below) and frozen for future culture in freezing medium composed of FBS plus 10% dimethyl sulfoxide (DMSO- Sigma). Isolated knock-in iPSC lines were frequently subcloned to ensure homogeneity of the population.

Transfection and CTS for Illumina MiSeq experiments – With the aim to assess the effect of our CTS regimen on editing outcomes, we carried out next-generation sequencing using the Illumina MiSeq platform via a pooled amplicon strategy, including 7 different variants of interest (Table S3) across 4 different genes (*CRYAB*, *BAG3*, *LMNA* and *MTERF4*,) in two different cell lines (hB53 hiPS6 and hB119 hiPS9). Samples were prepared as described above except, two days post-transfection (*day 2*), iPSCs were dispersed such that 10,000 iPSCs were allocated across 3 wells ($Puro^-$) and the remainder across the other 3 wells ($Puro^+$) of a 6-well plate with corresponding $Puro^-$ and $Puro^+$ groups derived from the same transfection. Media was changed every other day for 1 week (*day 5-12*) with or without puromycin, accordingly. Following 1 week maintenance (*day 12*), all three $Puro^+$ wells and all three $Puro^-$ wells were collected and combined separately. In order to deplete the feeder cell sub-population, cells were reseeded in one Matrigel-coated 6-well plate wells in mTeSR1 plus ROCK inhibitor. At confluence, cells were again dispersed, combined and pelleted for isolation of genomic DNA and library preparation for Illumina MiSeq analysis (see below).

Genotyping PCR and Sanger sequencing for clones

To isolate genomic DNA from clones, 30µl Quick Extract Solution (Epicentre) was added to each cell pellet (half colony) and incubated for 15 minutes at 65°C, followed by 5 minutes at 95°C. PCR was carried out using gene-specific primers (see below table) and the resulting amplicons were PCR-purified using a PureLink Quick PCR Purification Kit (Life Technologies) and Sanger sequencing was performed by Retrogen (San Diego, CA) with the same primers used for amplification. Sequences were analyzed using Sequencher software.

Primer Name	Primer Sequence (5'-3')
CRYAB_F	AGACAGTTATCTGTTGCTGAATGATATT
CRYAB_R	GGCAATTTCATCTTAGCTGCAA
BAG3_F	TGAAAGTGGAAGCCATCCTG
BAG3_R	GGCTGATCTGCTTCAAGGTT
LMNA_F	CCCCACTTGGTCTCCCTC
LMNA_R	GGCTCACCCTGGTCCACC
MTERF4_F	TTATATGCTTGCCTTTTTTGAA
MTERF4_R	GTCCGAGGCTTCTTATCCATAT

Illumina MiSeq library preparation

Genomic DNA was isolated from cell pellets using a PureLink Genomic DNA Mini Kit (Life Technologies). Samples were prepared for analysis with Illumina MiSeq as previously described (Kistler et al., 2015). PCR 1 primers are listed in the below table with adapter sequences in red and green text for the forward and reverse primers, respectively. PCR2 was performed using the Nextera XT Index Kit (#15055293) from Illumina according to manufacturer's instructions. Individual amplicons were quantified via qPCR (KAPA Biosystems) and pooled at 3nM concentrations. To ensure high sequencing quality, following pooling, final amplicon pools were quantitated by qPCR to determine the precise molarity of the pool as a whole. Samples were sequenced using Single read

sequencing (250bp read) and dual indexing on an Illumina MiSeq following the manufacturer's instructions. The pool was run with a 30% spike-in of Phi-X to avoid issues with low-complexity Amplicon Libraries.

Primer Name	Primer Sequence (5'-3')
CRYAB_MiSeq_F	TCGTCGGCAGCGTCAGATGTGTATAAGAGACAGCTGAGTTCTGGGCAGGTGAT
CRYAB_MiSeq_R	GTCTCGTGGGCTCGGAGATGTGTATAAGAGACAGTAATTTGGGCCTGCCCTTAG
BAG3_MiSeq_F	TCGTCGGCAGCGTCAGATGTGTATAAGAGACAGACCAAAGAGCTGCTGGCCCT
BAG3_MiSeq_R	GTCTCGTGGGCTCGGAGATGTGTATAAGAGACAGTCGCTGCTGCTGTGGCTTCT
LMNA_MiSeq_F	TCGTCGGCAGCGTCAGATGTGTATAAGAGACAGGCAGCAGCTTCTCACAGCAC
LMNA_MiSeq_R	GTCTCGTGGGCTCGGAGATGTGTATAAGAGACAGGGCACACGGATACCTTATCTTT
MTERF4_MiSeq_F	TCGTCGGCAGCGTCAGATGTGTATAAGAGACAGGGCAGAAAAGTTGAAGAATAGGTTT
MTERF4_MiSeq_R	GTCTCGTGGGCTCGGAGATGTGTATAAGAGACAGAGAAGTGCCTTTTCACGGTACA

Illumina MiSeq analysis methods

In all cases, reads were inspected using the FASTX-Toolkit to assess general quality and then 3'-clipped where the Q score in a 4 nucleotide sliding window fell below 15 and filtered as to retain only those of 100 nucleotides or longer using Trimmomatic (Bolger et al., 2014). Pipeline error rate was estimated by deep-sequencing unedited amplicons derived from each target gene and aligning FATSTQ-derived sorted/indexed BAM file to reference sequences (obtained from Ensembl release 84) with Bowtie2 and assessing sequence divergence in the informative segment (10 nucleotides up/downstream of the nucleotide to be mutated and the CRISPR PAM site) of each target read. Average coverage was ~240,000X and average sequence divergence from the reference at Q30 was 0.1%. For knock-in experiments, we quantified the extent of HDR-mediated donor integration by interrogating pre-processed FASTQ files (as described above) for informative segments of the donor sequence (typically ~50 nucleotides, spanning the targeted nucleotide and CRISPR cut site (not simply the targeted nucleotide, as this may occur in the presence of an indel and lead to overestimation of knock-in) using a Linux grep command (of format : grep -A 2 -B 1 'ssODN sequence' 'INPUT.FQ' | sed '/^--$/d' > 'OUTPUT.FQ') as well as via manual inspection of FASTQ files for confirmation. For comparative value, HDR was also quantified using the Church lab's CRISPR Genome Analyzer (Güell et al., 2014) and we observed good agreement with our estimates (data not shown).

Southern blotting

Southern blotting was performed to analyze zygosity of the *pac* cassette at the *AAVS1* locus and determine the rate of random integration. The probe was designed to the 5' homology arm (Figure S4b) and was digested from the SBI targeting vector using KpnI and ClaI restriction endonucleases (NEB) and radiolabeled. Genomic DNA was isolated from 48 puromycin resistant clones derived from transfection of the SBI targeting construct and TALENs followed by the CTS puromycin selection protocol. Southern blotting was performed based on previously described methods (Haque et al., 2000) with genomic DNA digested by EcoRV (NEB).

PCR-based assay for targeted and untargeted integration of the *AAVS1* donor construct

PCR to confirm HDR at *AAVS1* locus – As an independent confirmation of the Southern blotting data, the same 48 clones were screened with inside-out PCR using the SBI primers in the below table such that one falls inside the homology arm (i.e., in the exogenous sequence) and one falls outside (i.e., in the endogenous locus). Representative cell lines in Figure 3 were also screened in this way.

Name	Primer Sequence (5'-3')	Expected PCR Product Size
SBI 5' Forward	AGTCCGGACCACTTTGAGCTCTACT	1061bp
SBI 5' Reverse	GAGGAGTAGAAGGTGGCGCGAA	
SBI 3' Forward	AGGTTTAGCCCCGGAATTGACTG	1036bp
SBI 3' Reverse	CCAAAAGGCAGCCTGGTAGACA	
Transposagen 5' Forward	CTCTTTCCGGAGCACTTCC	711bp
Transposagen 5' Reverse	CCGATAAAACACATGCGTCA	

Transposagen 3' Forward	ACTTACCGCATTGACAAGCA	805bp
Transposagen 3' Reverse	CCAGATAGCACTGGGGACTC	

PCR to Screen for random integration of the *AAVS1* donor vector - To screen for random integration of the *AAVS1* donor construct, in addition to the Southern blot, three sets of PCR primers were designed for the SBI donor vector and two sets for the Transposagen vector that amplify the backbone region (i.e., the region of the vector outside of the homology arms) (see below table). PCR was performed using Accuprime Supermix II (Life Technologies) with plasmid DNA as a positive control and DNA from hB53 hiPS6 and hB119 hiPS9 iPSCs as negative controls. The same 48 clones from Southern blotting were screened in this way (Figure S4c). Internal primers were used as a control. Additionally, bands were undetectable in generated knock-in cell lines from Figure 3 (data not shown).

Vector	**Primer Name**	**Primer Sequence (5'-3')**	**Expected PCR Product Size**
SBI	Random F1	GTGCCACCTAAATTGTAAGCGTT	495bp
SBI	Random R1	AACAGTTGCGCAGCCTGAAT	
SBI	Random F2	TGCTGCTGCATTGACGTTGA	408bp
SBI	Random R2	TGCTTCCGGCTCGTATGTTG	
SBI	Random F3	CAACATACGAGCCGGAAGCA	412bp
SBI	Random R3	CCTCTGACTTGAGCGTCGATTT	
SBI	Internal F	ACCCCAGCATCCTGCAGAAC	445bp
SBI	Internal R	ACCCACACCTTGCCGATGTC	
Transposagen	Random F4	GCTTCCTCGCTCACTGACTC	409bp
Transposagen	Random R4	CGACCTACACCGAACTGAGA	
Transposagen	Random F5	CGGTGAAAACCTCTGACACA	380bp
Transposagen	Random R5	ATTCACTGGCCGTCGTTTTA	

Immunocytochemistry

Immunocytochemistry was performed as previously described (Mitzelfelt et al., 2016). Briefly, iPSCs were seeded onto 12mm glass coverslips in 12 well plates coated with Matrigel in mTeSR1 or StemMACS iPS-Brew XF supplemented with 10μM ROCK inhibitor. The following day, media was changed minus ROCK inhibitor and incubated for 4 hours. iPSCs on coverslips were washed with DPBS, fixed with 4% paraformaldehyde at room temperature for 15 minutes, washed two times with DPBS, and stored in DPBS at 4°C until staining. Cells were permeabolized with 0.1% triton-X 100 in DBPS for 10 minutes, washed once in DPBS, and blocked for 1 hour at room temperature with 3% bovine serum albumin (BSA-Sigma) in DPBS. Primary antibody was added in 3% BSA/DPBS and incubated for 2 hours at room temperature. Primary antibodies: Nanog (Cell Signaling 4903p, USA, 1:200) and stage-specific embryonic antigen-4 (SSEA-4) (Stem Cell Technologies 60062AD, USA, 1:40). Cells were washed three times with DPBS. Secondary antibody was added in DBPS and incubated for 1 hour at room temperature. Secondary antibody: Alexa Fluor 555 donkey anti-rabbit IgG (A31572). Cells were washed three times and mounted with Ultracruz Hard Set Mounting Media plus DAPI (Santa Cruz). Representative images were taken using the inverted Nikon Eclipse TE 2000.

Karyotyping

Karyotyping, performed as previously described (Mitzelfelt et al., 2016), was carried out by Wisconsin Diagnostic Laboratories (formerly Dynacare Laboratories), Milwaukee WI. Chromosomes of 20 proliferating cells were counted and fully analyzed using G-banding with representative images shown (Figure 3).

Potential off-target analysis

Clone Analysis: Potential off-target sites were predicted by CRISPR RGEN Tools Cas-OFFinder (Bae et al., 2014) and are shown in the below table (with lowercase text indicating mismatches from the guide sequence). We chose the top 3-5 off-target sites for each CRISPR guide and designed primers that amplify a 300-500bp region around the off-target site. Off-target genomic regions were amplified using Accuprime Supermix II in all isolated knock-in clones. Amplicons were PCR-purified using a PureLink Quick PCR Purification Kit and Sanger sequencing was

performed by Retrogen in both the 5' and 3' directions with the amplification primers. Sequences were analyzed using Sequencher software. Sequencing results were compared with the originating cell line (either hB53 hiPS6 or hB119 hiPS9). No mutations were noted (data not shown).

CRISPR	Potential Off-Target Site	Chromosome	Position	Primer Name	Primer Sequence (5'-3')
CRYAB	GaGATCCGGTAaTTCCTGAGG	chrY	17785850	OT_1_F	AGCATGCAGTTTAATCATTG
				OT_1_R	CCTATAATGTGTTGGGGAAA
	GGGATCCaGTAaTTCCTGAGG	chrY	18489869	OT_2_F	CAGCATGCAGTTCAATCAT
				OT_2_R	TATAACGTGTTGGGCAAAGT
	GGGATCCaGTAaTTCCTGTGG	chrY	23737276	OT_3_F	AGCCTGCAGTTCAATCAT
				OT_3_R	CATAAGGTGTTGGGCATATT
	GGGAaCaGGTATTTCCTGCGG	chr6	40874614	OT_4_F	TTCCTTGCTTTCTTCCTATG
				OT_4_R	AGGCCAGGGAAGTTAAAGTA
	GGGAaCCGcTATTTCCTGAGG	chrX	153640375	OT_5_F	GGTCTGACAGGAAACAAGAT
				OT_5_R	GGAGAAACATTTGGATTGAA
BAG3	GGGAaGAGCCAGATGgGgGTCAGG	chr12	53068310	OT_1_F	CAGCTCCATGAGCAAAAA
				OT_1_R	AAGTGTGTGGGGGAAGAC
	GGGAaGAGCaGATTGTGCGTaGGG	chr3	62611736	OT_2_F	CACAGAGCTTGGCTTCTAGT
				OT_2_R	CTACAAGGCCTTTGATGAGT
	GGGACGAGCCaATGTGCtTtAGG	chr7	57160206	OT_3_F	TCTGCATGTTGAAATTGTTT
				OT_3_R	TGGGAAAATTTTGGAGATTA
	GGcACGAGCTACcATGTcCGTCTGG	chr4	147603021	OT_4_F	CAATCCTCCCACCTTAGC
				OT_4_R	TCCTTTTATGCACCAAGTTT
LMNA	tATTGGACTTcTTGgGCAGCCGG	chr12	26116974	OT_1_F	CTAATGGTTTTAGCCCACAA
				OT_1_R	TCACATACAGCAAGCAAAAC
	CATgGGACTTGTTGCGtAGaTGG	chr10	6557892	OT_2_F	ATGTTTCAAAGCAAGGAAGA
				OT_2_R	CCCCTGTATTCAACTCCATA
	CAcTGGAaTTtTTGCtCAGCAGG	chr8	4084793	OT_3_F	AACACATTCACTTCCTTTGG
				OT_3_R	TTGGGAGAGAGAAAATGAAA
	CATTGGgCTgGTTGgGCAcCAGG	chr8	41681653	OT_4_F	TCCTATGTGGGAGAAGCA
				OT_4_R	TGTCCAGAATCAGCTTCTTT
	CATTGGgCTTaggGCGCAGCTGG	chr8	69992997	OT_5_F	AAGTCCAAAACGAAGGTGTT
				OT_5_R	CTGAGGCAGGAGAATCACT
MTERF4	ACcTGTATTCCAGTCTGAtCCTGG	chr12	115848234	OT_1_F	TTTTGAAATTGGGAGATGAG
				OT_1_R	TGAAGCTTTGTTCTTCCTGT
	cCTTGTAcTCCATGTTGACCCAGG	chr3	105899012	OT_2_F	CGTGTACTTTATCATTTAACAGC
				OT_2_R	GATCTGTGGACAGAAAGTCC
	ACTTtTATTCCAGcTGACCACAGG	chr5	53828304	OT_3_F	TCTTGTTTTACTGTGGCTGA
				OT_3_R	ATGGCTGTACAAAATTGAGC

Illumina MiSeq Analysis: To ensure CTS does not enrich for off-target effects, we chose our most active CRISPR (targeting *CRYAB*), and analyzed the top 12 potential off-target sites by deep-sequencing using the Illumina MiSeq. CRISPR RGEN Tools Cas-OFFinder (Bae et al., 2014) was used to identify potential off-target sites with sequences

identified in the below table (lowercase text indicates mismatches from the guide sequence). Primers were designed flanking these sites and samples were prepared and analyzed using the Illumina MiSeq (as described above). PCR 1 primers are listed in the table below (adapter sequences in red and green text for the forward and reverse primers, respectively). Reads were inspected and 3'-clipped as described above before being aligned to the appropriate off-target reference sequences using Bowtie2 (with the 'local' alignment setting to maximize the chance of finding indels). Resulting SAM files were converted to sorted/indexed BAM files and loaded into IGV for viewing. We found no measurable difference in indel presence between pooled populations following CTS compared to without CTS.

Potential Off-Target Site	**Chr**	**Position**	**Primer Name**	**Primer Sequence (5'-3')**
GaGATCCGGTAaT TCCTGAGG	chrY	17785850	COT_MS_F_1	TCGTCGGCAGCGTCAGATGTGTATAAGAGACAG CAGGCATGTTGTTGTTAATC*
			COT_MS_R_1	GTCTCGTGGGCTCGGAGATGTGTATAAGAGACA GTTAGCTGGAAATTGTGATCC*
GGGATCCaGTAaT TCCTGAGG	chrY	18489869	COT_MS_F_2	TCGTCGGCAGCGTCAGATGTGTATAAGAGACAG ATTCATCAACCAAGCAGGT*
			COT_MS_R_2	GTCTCGTGGGCTCGGAGATGTGTATAAGAGACA GCTTCAGCATTAGCTGGAAAT*
GGGATCCaGTAaT TCCTGTGG	chrY	23737276	COT_MS_F_3	TCGTCGGCAGCGTCAGATGTGTATAAGAGACAG CAAGCAGGTTGTTGTAGTCA*
			COT_MS_R_3	GTCTCGTGGGCTCGGAGATGTGTATAAGAGACA GCTTCAGCATTAGCTGGAAAT*
GGGATCCaGTAaT TCCTGAGG	chrY	23941131	COT_MS_F_4	TCGTCGGCAGCGTCAGATGTGTATAAGAGACAG TAAGCAGGTTGTTGTTGTCA*
			COT_MS_R_4	GTCTCGTGGGCTCGGAGATGTGTATAAGAGACA GCTTCAGCATTAGCTGGAAAT*
GGGAaCaGGTAT TTCCTGCGG	chr6	40874614	COT_MS_F_5	TCGTCGGCAGCGTCAGATGTGTATAAGAGACAG GACCCTGTGTGAGACAGAAA
			COT_MS_R_5	GTCTCGTGGGCTCGGAGATGTGTATAAGAGACA GGTGCCTTCTCATAGGGAAT
GGGAaCCGcTATT TCCTGAGG	chrX	153640375	COT_MS_F_6	TCGTCGGCAGCGTCAGATGTGTATAAGAGACAG CCAAGCAAACTTGCACTC
			COT_MS_R_6	GTCTCGTGGGCTCGGAGATGTGTATAAGAGACA GAAAGGCTTGGTGGGTGAG
GGtATCCtGTATT TCCTcTGG	chr8	41832706	COT_MS_F_7	TCGTCGGCAGCGTCAGATGTGTATAAGAGACAG TATTGCACAGGACAGACTTG
			COT_MS_R_7	GTCTCGTGGGCTCGGAGATGTGTATAAGAGACA GCAGCAGATGTTAGGTCAGAA
GaGATCaGGTAcT TCCTGGGG	chr8	120828204	COT_MS_F_8	TCGTCGGCAGCGTCAGATGTGTATAAGAGACAG GTGCTCTTTGTTCTGAAGGA
			COT_MS_R_8	GTCTCGTGGGCTCGGAGATGTGTATAAGAGACA GCAGTGTTGACAAGCATCTGA
GGGATCaGGTgTT TCtTGTGG	chr12	128299314	COT_MS_F_9	TCGTCGGCAGCGTCAGATGTGTATAAGAGACAG AGACCAGCTCATCTTTTCAA
			COT_MS_R_9	GTCTCGTGGGCTCGGAGATGTGTATAAGAGACA GGGTATTTAACGCTGAGAGCA
aGaATCtGGTATT TCCTGTGG	chr3	123694853	COT_MS_F_10	TCGTCGGCAGCGTCAGATGTGTATAAGAGACAG AGGCAGCTTTTCCAACCT
			COT_MS_R_10	GTCTCGTGGGCTCGGAGATGTGTATAAGAGACA GCCTATAGCAGAGCCTCCAG
GaGATtCGGTcTT TCCTGAGG	chr3	179083191	COT_MS_F_11	TCGTCGGCAGCGTCAGATGTGTATAAGAGACAG GCATGGACATCTGACCTACT
			COT_MS_R_11	GTCTCGTGGGCTCGGAGATGTGTATAAGAGACA GTGGGAGATTAGAATGTTGCT
GGGAaCaGGgATT TCCTGCGG	chr7	45889831	COT_MS_F_12	TCGTCGGCAGCGTCAGATGTGTATAAGAGACAG GGAGGAATTAGGACTTCCAT
			COT_MS_R_12	GTCTCGTGGGCTCGGAGATGTGTATAAGAGACA GTCAGCTTCTCCATCCTTAAA

*Primers amplified >1 locus with same sequence

Supplemental References

Bae, S., Park, J., and Kim, J.-S. (2014). Cas-OFFinder: a fast and versatile algorithm that searches for potential off-target sites of Cas9 RNA-guided endonucleases. Bioinformatics *30*, 1473-1475.

Bolger, A.M., Lohse, M., and Usadel, B. (2014). Trimmomatic: a flexible trimmer for Illumina sequence data. Bioinformatics *30*, 2114-2120.

Chen, F., Pruett-Miller, S.M., Huang, Y., Gjoka, M., Duda, K., Taunton, J., Collingwood, T.N., Frodin, M., and Davis, G.D. (2011). High-frequency genome editing using ssDNA oligonucleotides with zinc-finger nucleases. Nature methods *8*, 753-755.

Cong, L., Ran, F.A., Cox, D., Lin, S., Barretto, R., Habib, N., Hsu, P.D., Wu, X., Jiang, W., Marraffini, L.A.*, et al.* (2013). Multiplex Genome Engineering Using CRISPR/Cas Systems. Science *339*, 819-823.

Dialynas, G., Flannery, K.M., Zirbel, L.N., Nagy, P.L., Mathews, K.D., Moore, S.A., and Wallrath, L.L. (2012). LMNA variants cause cytoplasmic distribution of nuclear pore proteins in Drosophila and human muscle. Human Molecular Genetics *21*, 1544-1556.

Forrest, K.M.L., Al-Sarraj, S., Sewry, C., Buk, S., Tan, S.V., Pitt, M., Durward, A., McDougall, M., Irving, M., Hanna, M.G.*, et al.* (2011). Infantile onset myofibrillar myopathy due to recessive CRYAB mutations. Neuromuscular Disorders *21*, 37-40.

Geurts, A.M., Cost, G.J., Freyvert, Y., Zeitler, B., Miller, J.C., Choi, V.M., Jenkins, S.S., Wood, A., Cui, X., Meng, X.*, et al.* (2009). Knockout Rats via Embryo Microinjection of Zinc-Finger Nucleases. Science *325*, 433-433.

Güell, M., Yang, L., and Church, G.M. (2014). Genome editing assessment using CRISPR Genome Analyzer (CRISPR-GA). Bioinformatics *30*, 2968-2970.

Haque, J., Boger, S., Li, J., and Duncan, S.A. (2000). The Murine Pes1 Gene Encodes a Nuclear Protein Containing a BRCT Domain. Genomics *70*, 201-210.

Hockemeyer, D., Wang, H., Kiani, S., Lai, C.S., Gao, Q., Cassady, J.P., Cost, G.J., Zhang, L., Santiago, Y., Miller, J.C.*, et al.* (2011). Genetic engineering of human pluripotent cells using TALE nucleases. Nat Biotech *29*, 731-734.

Kistler, Kathryn E., Vosshall, Leslie B., and Matthews, Benjamin J. (2015). Genome Engineering with CRISPR-Cas9 in the Mosquito Aedes aegypti. Cell Reports *11*, 51-60.

Long, C., McAnally, J.R., Shelton, J.M., Mireault, A.A., Bassel-Duby, R., and Olson, E.N. (2014). Prevention of muscular dystrophy in mice by CRISPR/Cas9–mediated editing of germline DNA. Science *345*, 1184-1188.

Miller, J.C., Holmes, M.C., Wang, J., Guschin, D.Y., Lee, Y.-L., Rupniewski, I., Beausejour, C.M., Waite, A.J., Wang, N.S., Kim, K.A.*, et al.* (2007). An improved zinc-finger nuclease architecture for highly specific genome editing. Nat Biotech *25*, 778-785.

Mitzelfelt, K.A., Limphong, P., Choi, M.J., Kondrat, F.D., Lai, S., Kolander, K.D., Kwok, W.M., Dai, Q., Grzybowski, M.N., Zhang, H.*, et al.* (2016). Human 343delT HSPB5 Chaperone associated with Early-onset Skeletal Myopathy causes Defects in Protein Solubility. J Biol Chem.

Norton, N., Li, D., Rieder, Mark J., Siegfried, Jill D., Rampersaud, E., Züchner, S., Mangos, S., Gonzalez-Quintana, J., Wang, L., McGee, S.*, et al.* (2011). Genome-wide Studies of Copy Number Variation and Exome Sequencing Identify Rare Variants in BAG3 as a Cause of Dilated Cardiomyopathy. The American Journal of Human Genetics *88*, 273-282.

Paquet, D., Kwart, D., Chen, A., Sproul, A., Jacob, S., Teo, S., Olsen, K.M., Gregg, A., Noggle, S., and Tessier-Lavigne, M. (2016). Efficient introduction of specific homozygous and heterozygous mutations using CRISPR/Cas9. Nature *advance online publication*.

Ponce de León, V., Mérillat, A.-M., Tesson, L., Anegón, I., and Hummler, E. (2014). Generation of TALEN-Mediated GR^{dim} Knock-In Rats by Homologous Recombination. PLoS ONE *9*, e88146.

Richardson, C.D., Ray, G.J., DeWitt, M.A., Curie, G.L., and Corn, J.E. (2016). Enhancing homology-directed genome editing by catalytically active and inactive CRISPR-Cas9 using asymmetric donor DNA. Nat Biotech *34*, 339-344.
Riedel, M., Jou, Chuanchau J., Lai, S., Lux, Robert L., Moreno, Alonso P., Spitzer, Kenneth W., Christians, E., Tristani-Firouzi, M., and Benjamin, Ivor J. (2014). Functional and Pharmacological Analysis of Cardiomyocytes Differentiated from Human Peripheral Blood Mononuclear-Derived Pluripotent Stem Cells. Stem Cell Reports *3*, 131-141.
Sacconi, S., Féasson, L., Antoine, J.C., Pécheux, C., Bernard, R., Cobo, A.M., Casarin, A., Salviati, L., Desnuelle, C., and Urtizberea, A. (2012). A novel CRYAB mutation resulting in multisystemic disease. Neuromuscular Disorders *22*, 66-72.
Vicart, P., Caron, A., Guicheney, P., Li, Z., Prevost, M.-C., Faure, A., Chateau, D., Chapon, F., Tome, F., Dupret, J.-M*., et al.* (1998). A missense mutation in the [agr]B-crystallin chaperone gene causes a desmin-related myopathy. Nat Genet *20*, 92-95.
Villard, E., Perret, C., Gary, F., Proust, C., Dilanian, G., Hengstenberg, C., Ruppert, V., Arbustini, E., Wichter, T., Germain, M*., et al.* (2011). A genome-wide association study identifies two loci associated with heart failure due to dilated cardiomyopathy. European Heart Journal *32*, 1065-1076.